



THE IMPACT OF MOTIVATIONAL FACTORS ON JOB SATISFACTION OF PUBLIC AND PRIVATE SECTOR BANK EMPLOYEES

Dr. Ishita Chatterjee¹, Manaswini Chattopadhyay²

¹*Assistant Professor, Department of Applied Psychology, University of Calcutta, (India)*

²*M. Sc. In Applied Psychology, University of Calcutta, (India)*

ABSTRACT

The present study was conducted with a view to assess the impact of motivational factors on job satisfaction of public and private sector bank employees. The focus of the study was to find out whether there was any significant difference between public & private sector banks employees regarding their perception of intrinsic & extrinsic motivational factors and job satisfaction whether there was any significant relationship between motivational factors (intrinsic & extrinsic) & job satisfaction among the employees of public & private sector banks. The sample consisted of 30 public and 30 private sector bank employees. Random sampling technique was used for sample selection. General information schedule, job satisfaction scale, motivational (intrinsic & extrinsic) scale were administered to them. Mean, standard deviation, t-test, Person's Product Moment correlation were used for statistical analyses. Result revealed that there was a significant difference between public & private sector bank employees regarding their perception of motivational factors (intrinsic & extrinsic) & job satisfaction. The statistical analysis also showed that there was a significant correlation between motivational factors (intrinsic & extrinsic) & job satisfaction.

Both organization & employee could use these finding of this present study for better outcome.

Keywords : Job Satisfaction, Motivation, Private And Public Sector Bank Employees.

I. INTRODUCTION

Job satisfaction & work motivation are key concepts for the prosperity of any organization & its workers. Workers who are motivated toward their job feel more satisfaction in their jobs. They gave their best efforts & work with the full potential they possess. They have a feeling of completeness & are very happy with their job. Thus work motivation & job satisfaction are becoming the key issue of research in organizational behaviour.

Public sector can be defined as the part of economy concerned with providing basic government services. The public sector includes the banking system of the country. Public Sector Banks (PSBs) are banking where a majority stake (more than 50%) is held by government. Private sector can be defined as all economic activity other than that of government. Private sector banks are banks where greater parts of stake or equity are held by the private shareholders & not by the government.

The term motivation is derived from the Latin word 'movere' which means to be moved to do something (Steer et. al., 2004).



According to Latham & Pinder, 2005; Motivation is also consider as the interaction between the individual & the situation or environment.

Jenica (2007), "Motivation is inferred from a systematic analysis of how personal task & environmental characteristics influence behaviour & job performance".

After reviewing all the related definitions motivation is defined as "a force that originates individuals to take action to accomplish personal & organizational goals". Individuals have not only different amounts, but also different kinds of motivation with respect to environments culture (Awaremi et. al, 2011).

According to McCormick & Tiffin (1979) motivation can either be intrinsic or extrinsic. According to Zhang (2010) intrinsic motivation is one of the most appropriate & strong influence on workers creativity. Ryan & Deci (2000) consider intrinsic motivation to be the most important & pervasive motivation.

II. INTRINSIC MOTIVATIONAL FACTORS

Interesting work

Job appreciation

Job satisfaction

Stress

An intrinsically motivated individual according to Ajila (1997) will be committed to his work to the extent to which the job inherently contains task that are rewarding to him or her.

Individuals are extrinsically motivated when they engage in the work in order to obtain some goal that is apart from the work itself (Amabile, 1996). Extrinsic motivation is provided to employee because it is an effortless solution for task fulfillment.

III. EXTRINSIC MOTIVATIONAL FACTORS

Job security

Good Wages

Promotion & Growth

Recognition

Khalid, Salim & Loke (2011) conducted a study on impact of reward & motivation on job satisfaction in Water Utility Industry in Malaysia. Result revealed that reward has a positive influence on motivation & job satisfaction of public sector employees.

A study conducted by Delbert M. Nebeker & Charles Tantum (2006) on 62 computer operators showed motivational factors had varying effects on job satisfaction.

Akanbi (2002) conducted a research on influence of intrinsic & extrinsic motivation on job satisfaction. The findings revealed positive relationship between intrinsic motivation & job satisfaction.

A study conducted by Robert B. Edwin, Patricia C. Smith & Charles L. Hulin (1966) on 793 employees from various jobs showed that intrinsic motivational factors were more strongly related to job satisfaction than extrinsic motivational factors.

A study conducted by Leach (1991) & Westbreak (2000) on public & private sector employees showed that results tended to emphasize more impact of intrinsic motivational fators on job satisfaction in both sectors.



Job satisfaction is a positive emotional state that occurs when a person's job seems to fulfill important values, provided these values are compatible with one's needs.

The relevance of the job satisfaction among bank employees to the overall bank performance becomes even more important under the challenging condition associated with the global recession, especially due to the accompanying increase in non-performing loans (NPLs) & the cost of provisions for potential losses associated with credit, as well as the consequent fall in profitability.

Vroon (1964) defined job satisfaction as an affective orientation on the part of the individuals toward work roles which they are presently occupying.

Armstrong (2006) defined job satisfaction as an attitude & feelings people have about their work. Positive & favourable attitudes towards the job indicate job satisfaction. Negative & unfavourable attitude towards the job indicate job dissatisfaction.

IV. FACTORS OF JOB SATISFACTION

Person Factors – Worker's sex, age, education, marital status etc.

Factors inherent in the job – Work itself, condition etc.

Factors controlled by management – Nature of supervision, job security, kind of work, group, wage rate etc.

V. DETERMINANTS OF JOB SATISFACTION

5.1 Organizational Variable

The work itself

Skill variety

Task identity

Task significance

Autonomy

Feedback from the job itself

Pay

Supervision

Promotion

Work group

Working condition

Time on job

Size of plant

5.2 Personal Variable

Age

Sex

Intelligence

Job experience

Personality



VI. NUMBER OF DEPENDENTS

Yasir Hussan, Kashifuddin, Zark Mir, Khalil Ahmed, Abdul Mateem, Waseem Ahmed & Ahmed Bilal Nasir (2011) conducted a study to examine the job satisfaction level in private banking sector in Pakistan. The result revealed that most of the employees working in private banks are satisfied with their work management functions & job position.

Arunima Srivastava & Pooja Purang (2009) conducted a study on employee perception of job satisfaction : a comparative study on Indian Banks. Results revealed that private sector bank employees report greater satisfaction with pays benefit aspect & the public sector bank employees are more satisfied in respect of job security.

Sharma & Kumari (2004) found that public sector employees are more dissatisfied with their working condition & incentive than employees of private sector.

In a study on work ethics of industrial work force in selected private & public sector enterprise in Kerala, Wilson (2003) found that workers in private sector are not satisfied with reward system as compared to their counterparts in public sector.

6.1 Objectives

To study the difference between public and private sector bank employees regarding their perception of motivational factors (intrinsic & extrinsic) & job satisfaction.

To study the relationship between motivational factors (intrinsic & extrinsic) & job satisfaction among public & private sector bank employees.

6.2 Hypotheses

Hypothesis 1 : There is no significant difference between public & private sector bank employees regarding their perception of (intrinsic & extrinsic) motivational factors.

Hypothesis 2 : There is no significant difference between public & private sector bank employees regarding their perception of job satisfaction.

Hypothesis 3 : There is no significant relationship between motivational factors (intrinsic & extrinsic) & job satisfaction of both public & private sector bank employees.

VII. METHOD

7.1 Sample

Random sampling technique was used. Total sample size was 60 (30 employees including both male & female for public sector, bank and 30 employees including both male & female for private sector bank). Participants were chosen from age group of 25 – 45 year, with minimum educational qualification was graduation. All the subjects belonged to the middle & upper middle class section of the society in Kolkata.

For public sector banks, employees of SBI, Corporation Bank, BOI, UCO Bank, who were working in around Kolkata were selected.



For private sector banks, employees of Axis Bank, ICICI Bank, HDFC Bank & Kotak Mahindra Bank who were working in & around Kolkata were selected. The exclusion criteria were –

- Professionals not willing to answer the entire questions were not included for the present study.
- Professionals with past psychiatric illness were not included.

7.2 Tools

Job satisfaction scale was developed by Warr et. al. (1979). It is a self-administering questionnaire & there is no time limit. It is a 5 point Likert type scale (1 = extremely dissatisfied, 5 = extremely satisfied). Reliability of the scale was verified & found to be 0.78.

Motivational scale was constructed by U. Pareek (1996). This instrument contained 14 items, 7 related to intrinsic & 7 related to extrinsic motivation. It is self administering questionnaire. & respondents are asked to rank order 14 items depending on their importance to them from 1(highest rank) to 14(lowest rank). The lower the score the higher is the given value to the concerned factor. Reliability was 0.88.

7.3 Statistical Analysis

After data collection & scoring the data put to statistical analyses. Mean, SD, t-test, Product Moment Correlation were calculated.

VIII. RESULTS & DISCUSSION

Table .1 Comparison Between Public & Private Sector Bank Employees Regarding Their Perception of Intrinsic & Extrinsic Motivational Factors.

Motivational Factors	Public Sector Bank		Private Sector Bank		t value	Comments
	Mean	Standard Deviation	Mean	Standard Deviation		
Intrinsic	43.03	7.29	58.10	7.83	7.708**	Significant at 0.01 level
Extrinsic	61.56	7.77	46.13	9.27	6.973**	Significant at 0.01 level

* Significant at 0.05 level

** Significant at 0.01 level

From the above table, it was found that mean for intrinsic motivational factors was 43.03 for public sector bank employees & the mean score for private sector bank employees was 58.10. The significance of differences or t value between the public sector bank employees & private sector bank employees regarding their perception of intrinsic motivational factor was 7.708 which is significant at 0.01 level of significance. So, it can be said that there was a significant difference between public & private sector bank employees regarding their perception of intrinsic motivational factor. However, since high scores on intrinsic motivational factors mean low intrinsic motivation, so it can be said that public sector bank employees had higher intrinsic motivation than private sector bank employees. Wilson (2003) found that workers in private sector were not satisfied with reward as compared to their counterparts in public sector.



The mean score for extrinsic motivational factors in case public & private sector bank employees were 61.56 & 46.13 respectively. The significant difference or t – value between the public sector bank employees and private sector bank employees regarding their perception of extrinsic motivational factor was 6.973, which is significant at 0.01 level. So, it can be said that there was a significant difference between public & private sector bank employees regarding their perception of extrinsic motivational factor. Since high score indicated lower extrinsic motivation, it can be interpreted that private sector bank employees had higher extrinsic motivation public sector bank employees.

Sharma & Kumari (2004) found that public sector employees were more dissatisfied with their working condition & incentives than employees of private sector.

Table 2 Comparison Between Public & Private Sector Bank Employees Regarding Their Perception of Job Satisfaction.

Sector	Mean	Standard Deviation	t – value	Comments
Public	65.20	8.33	2.428*	Significant at 0.05 level
Private	70.26	7.83		

* Difference is significant at 0.05 level

From the above table it was found that mean for job satisfaction was 65.20 for public sector bank employees & 70.26 for private sector bank employees. The significance of difference or t value between public & private sector bank employees regarding their perception of job satisfaction was 2.428 which was significant at 0.05 level. The null hypothesis was rejected. So, there was a significant difference between public & private sector bank employees regarding their perception of job satisfaction. It was also found that private sector bank employees had greater job satisfaction than public setor bank employees. Yasir Hussan, Khashifuddin, Zark Mir, Khalil Ahmed, Abdul Mateem, Waseen Ahmed & Ahmed Belal Nasir (2011) found that most of the employees in private banks were satisfied with their work management functions & job positions. Arunima Srivastava & Pooja Purang (2009) found that private sector bank employees report greater satisfaction with pay & benefit aspect & public sector bank employees were more satisfied in respect of job security.

Table 3 Relation Between Motivational Factors (Intrinsic & Extrinsic) & Job Satisfaction as Perceived by Both Sector of Bank Employees.

Variables		Obtained correlation Pearson's Product Moment Correlation	Comments
Intrinsic	Job Satisfaction	0.326*	Significant at 0.05 level
Extrinsic	Job Satisfaction	-0.325*	Significant at 0.05 level

The table showed that correlation between intrinsic motivational factors score & job satisfaction was 0.32 which was significant at 0.05 level. This reflected that as score on intrinsic motivational factor increased the score on job satisfaction also increased. This table also showed that correlation between extrinsic motivational factor & job satisfaction was -0.325 which was significant at 0.05 level so it might be concluded that there exists a negative correlation between extrinsic motivation & job satisfaction. Leach (1991) & Westbrook (2000) found that both public & private sector employees emphasized more impact of intrinsic motivational factors on job satisfaction. Aknabi (2002) found a positive relationship between intrinsic motivation & job satisfaction.



IX. CONCLUSION

From the present study it was concluded that there was a significant difference between public & private sector bank employees regarding their perception of motivational factors (intrinsic & extrinsic) & job satisfaction. Intrinsic motivation was found to be more in case of public sector bank employees & extrinsic motivation was found to be more in case of private sector employees. There was a significant positive correlation between intrinsic motivation & job satisfaction & there was a significant negative relationship between extrinsic motivation & job satisfaction among both public & private sector bank employees.

8.1 Limitations

- ⇒ Small sample size was a major limitation of this study.
- ⇒ Gender difference was not considered in this study because numbers of female respondents were very less than male respondents.
- ⇒ A number of questionnaires were used in this study. However, questionnaire may invite falsification & faking behaviour on the part of the subjects. A tendency towards subjective bias may also be present when questionnaire were used. Indirect test like projective test should be administered to overcome this limitation.
- ⇒ Time constrain was a major limitation as it had to be completed in a short period of time.

X. ADVANTAGES AND APPLIED VALUE OF THIS WORK

The study of job satisfaction among bank employees was important because there are various aspects of job that are highly attractive & lead to satisfaction & aspect of job that lead to dissatisfaction. Findings of this study provide instruction to employers who are concerned about customer satisfaction & maximize banking operations efficiently & effectively. Some important implication were –

Banking sector will be equipped with useful information regarding satisfaction & motivation, which help to formulate policies accordingly.

Both organizations & employees can use these finding of the study for better outcome.

Organization can develop jobs/profile & conditions of employment around these findings ensuring employee satisfaction.

It is very clear that bank grows through financial reliability & maximization of their investments, therefore, employee work motivation is very appropriate for the excellence of banking operations & productivity.

REFERENCES

Journal Papers

- [1] Hussain, Yasir et. al. (2011), Job satisfaction in private banking sector of Pakistan. *Global Journal of Management and Business Research*; 11(12).
- [2] Srivastava Arunima, Purang Pooja (2009); Employee Perception of Job satisfaction : Comparative Study on Indian Banks. *Asian Academy of Management Journal*, 14(2), 65 – 78.
- [3] Sharma, S. K. & Kumari (2004); *Job satisfaction of the employees*, *Sajosp*s, 4(2), 64 – 67.



- [4] Delbert, M. Nebeker; B. Charles Tantum (1993), The effect of computer Monitoring, Standards & Rewards on Work Performance, Job satisfaction & stress. *Journal of Applied Psychology*, 27(7), 508 – 536.
- [5] Amabute, T. M., Conti, R. Coon, H, Larenby, J. & Hoorn, M. (1996), ‘Assessing the work environment for creativity’, *Academy of Management Journal*, 39(5), 1154 – 1184.
- [6] Leach Fredrick J. & Westbrook Jerry D. (2000), *Engineering Management Journal*, 12(4).
- [7] Tyilana, Xolani E. (2005). The impact of motivation on job satisfaction amongst employees of a national broadcaster, *Business Management Journal*, 10(5), 88.

Books

- [8] Charles D. Speilberger (2004). Encyclopedia of Applied Psychology, Elsevier Academic Press, Amsterdam.
- [9] Deci, L. E. & Ryan, R. M. (2000). Intrinsic & Extrinsic motivation : Classic definition & new direction, contemporary educational psychology, Plenum Press, New York, (25), 54 – 67.
- [10] Guilford J. P. (1987), Psychometric Methods, Tata McGraw Hill, New Delhi, Pg. – 379 – 387.
- [11] McCornick, E. J. & Tiffin, J. (1974), Industrial Psychology, Prentice Hall.
- [12] Garret, E. Henry (2009), Statistics in Psychology & Education; Paragon International Publishers, New Delhi.
- [13] Robins (2013), Organizational Behaviour, Pearson Education Inc.publishing as Prentice Hall, New Delhi.
- [14] Udai Pareek (2004), Understanding Organizational Behavioiur, Oxford University Press, New York.
- [15] Wilson O. (2003); Work ethics of the Industrial work force, a study with reference to selected public & private sector enterprises in Kerala. Ph. D. Thesis, University of Kerala, Thiruvananthapuram.

Website:

[www://on.wikipedia.org/wiki/Motivation](http://www.on.wikipedia.org/wiki/Motivation)
[www://en.wikipedia.org/wiki/jobsatisfaction](http://www.en.wikipedia.org/wiki/jobsatisfaction)
www.businessdictionary.com



NUMERICAL INVESTIGATION ON STRUCTURE OF A PARTIALLY PREMIXED METHANE FLAME AT VARIOUS EQUIVALENCE RATIOS

K. B. Sahu¹, P. Ghose², Natabar Mohapatra³, Manas Kumar Puthal⁴

¹*Professor, ²Asst. Professor, ^{3,4}M. Tech. Student, School of Mechanical Engineering, KIIT University, Bhubaneswar, (India)*

ABSTRACT

A numerical investigation on the prediction of temperature, major species (CH_4 , CO_2 , CO , H_2O , N_2 , O_2) from methane/air partially premixed flames are obtained for different primary equivalence ratios (ϕ). A computational model for an axi-symmetric partially premixed flame has been developed. Standard $k-\epsilon$ model is used to simulate the turbulent quantities. Different species transport equations are solved for different species followed by Fick's law. In order to predict the soot, Brookes and Moss soot model has been incorporated along with modified model constants through a developed precursor correlation. Discrete ordinate (DO) radiation model is employed to include the radiation effect throughout the flow field. The governing equations are solved by using ANSYS Fluent 14.0. The pressure based steady solver has been used to solve 2-D geometry in Cartesian co-ordinate system. When the equivalence ratio increases, the flame height observed to increase. The exact flame height is ascertained from the axial distributions of temperature and different species. The soot in the flame of equivalence ratio $\phi=1.48$ is negligibly small and distributed in a very small area along the axis. The formation of soot in the flames is higher with increase in equivalence ratio.

Keywords: Equivalence ratio, Partially premixed flames, Soot, Species.

I. INTRODUCTION

A partially premixed flame is formed when a rich mixture of fuel and air in a primary stream interacts with a lean mixture of fuel and air or air only in secondary stream. When correct premixing conditions are placed, then the partially premixed flames creates a lesser amount of pollution and are more steady. Several examples are present in the field of partially premixed flames such as, industrial furnaces, flames in gas turbine combustion chambers, spray flames, direct injection automobile engines, Bunsen flames, etc. Modern gas turbine combustion systems originally manufactured for non-premixed mode of combustion is prone to partial premixing due to geometric features are the best example for this kind. Partial premixed mode has advantage over non-premixed and premixed modes. Non-premixed combustion regime has the drawback of attaining high temperatures which effects the emission formation like NO. On the other end, lean premixed combustion is prone to generate combustion instabilities with high pressure fluctuations. Many works have been carried out with methane as the fuel in gaseous partially premixed flames. Because, methane has the large contribution to the natural gas for the practical applications. T. K. Mishra et al. [1] have experimentally investigated the species

concentration distribution in a partially premixed methane/air flame established on a axi-symmetric coaxial burner. The flame structures of laminar partially premixed flames of two different fuels (methane and propane) have also been compared by them [2]. Gore and Zhan [3] have experimentally investigated the NO_x emission and concentration of major species in a laminar partially premixed flame taking methane as the fuel in a co-flow central tube burner. The temperature and CO concentrations have been measured by Datta et al. [4] in a methane partially premixed flame in a co-flow burner using Coherent Anti-strokes Raman Scattering (CARS) method. Mokhov and Levensky [5] have measured temperature and the NO concentration in the burnout area of a methane partially premixed flame in a co-flow ceramic burner with upstream heat loss by using techniques of CARS and LIF respectively. Six co-flowing laminar, partially premixed methane/air flames have been investigated computationally and experimentally [6] to determine the fundamental effects of partial premixing by varying the primary equivalence ratio from ∞ (nonpremixed) to 2.464. Claramunt et al [7] have analyzed, by means of detailed numerical simulations, the influence of the partial premixing level and the adequacy of different mathematical submodels on the modelling of co-flow partially premixed methane-air laminar flames. The partially premixed methane/air flame have been investigated by Gicquel [8] in a two-dimensional configuration. The configuration was close to those used in real domestic boilers. Bennet et al [9] have studied on six co-flowing laminar ethylene/air flames, by varying the primary equivalence ratio from infinity (nonpremixed) to 3, to determine the fundamental effects of partial premixing. In the present work, five methane/air partially premixed flames of various equivalence ratios and a methane non-premixed flame are investigated to study the effect of equivalence ratios on the temperature and major species (CH_4 , CO_2 , CO, H_2O , N_2 , O_2) distribution. Two partially premixed flames of same equivalence ratio and different primary jet velocities are considered to study the influence of jet velocity.

II. SPECIFICATION AND GEOMETRY OF THE PROBLEM

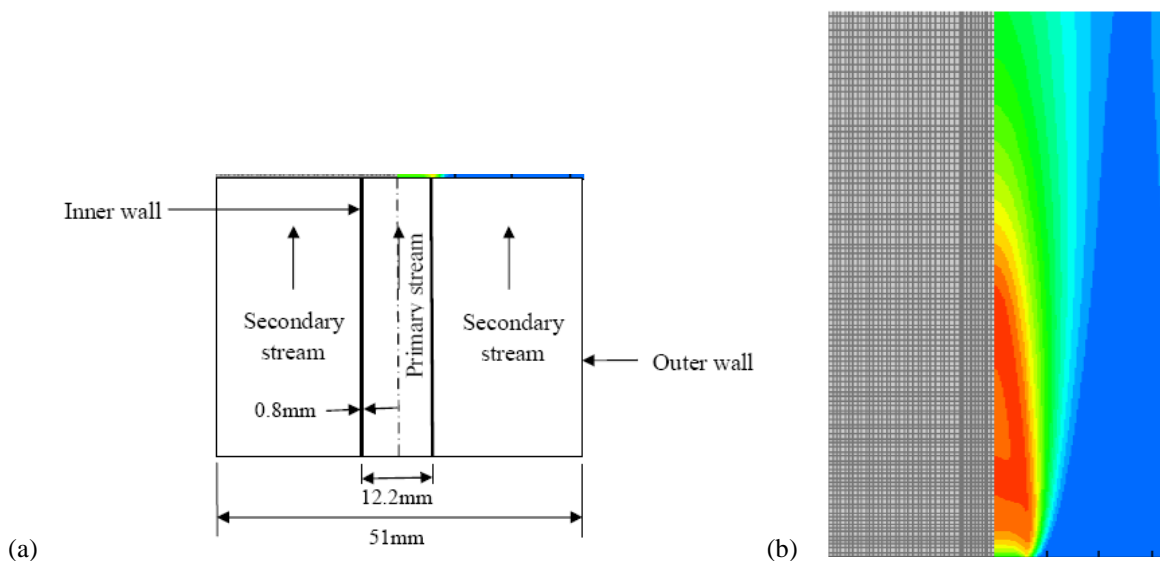


Figure 1. (a) Physical and (b) Meshed Computational Domain

2.1 Physical and Computational Domain

Fig. 1 shows the physical and meshed computational domain for the combustion in an axi-symmetric burner. The internal tube is of diameter 12.2 mm and thickness 0.8 mm where as the outer tube is of 51 mm diameter. The fuel-air mixture enters through the inner tube and secondary air flows through the outer annular space. The flame is produced above the burner. As the physical domain is symmetrical about the axis of the burner, the computational domain is taken half of the physical domain.

2.2 Operating Conditions and Boundary Conditions

In the present work, six flames have been studied. The operating condition of each flame is tabulated in TABLE 1. The first five flames are partially premixed flame where as the sixth flame is a non-premixed flame. The required fuel and air velocities to achieve these operating conditions are tabulated in TABLE 2.

The outer surface is assumed to be the adiabatic wall with no slip condition. At the entrance of the inner tube, the primary jet velocity is given as the velocity inlet to that face. At the outlet, the atmospheric pressure is given as the pressure boundary condition. Similarly, the secondary velocity is given as the velocity inlet to the appropriate face.

Table 1. Operating Conditions

Run No.	Fuel flow rate (l/min)	Primary premixing air flow rate (l/min)	Secondary co-flow air flow rate (l/min)	Primary jet velocity (m/s)	Secondary velocity (m/s)	Primary equivalence ratio
1	0.56	3.6	40	0.5931	0.3521	1.48
2	0.56	3.0	40	0.5075	0.3521	1.77
3	0.56	2.5	40	0.4362	0.3521	2.13
4	0.56	1.7	40	0.3222	0.3521	3.14
5	0.9	2.73	40	0.5175	0.3521	3.14
6	0.56	0	40	0.0798	0.3521	∞

Table 2. Boundary Conditions for ANSYS Fluent

Run No.	Inlet Air Velocity (m/s)	Inlet fuel Velocity (m/s)	Mass fraction of CH ₄	Mass fraction of O ₂	Primary Equivalence Ratio
1	0.3521	0.5971	0.077621	0.212147	1.48
2	0.3521	0.5075	0.091721	0.208904	1.77
3	0.3521	0.4362	0.108033	0.205141	2.13
4	0.3521	0.3222	0.151252	0.195212	3.14(0.56)
5	0.3521	0.5175	0.151353	0.195189	3.14(0.9)
6	0.3521	0.0798	1	0	∞

Turbulent intensity = 5 %

Turbulent length scale (m) = 0.00357 m

III. RESULT AND DISCUSSIONS

The species and temperature distribution within a partially premixed flame depends on the equivalence ratio of fuel air mixture and the velocity of the mixture. In the present study different partially premixed flames and a nonpremixed flame are taken to see the species and temperature distribution within the flame. The results are obtained and discussed as follows:

3.1 Temperature Contours

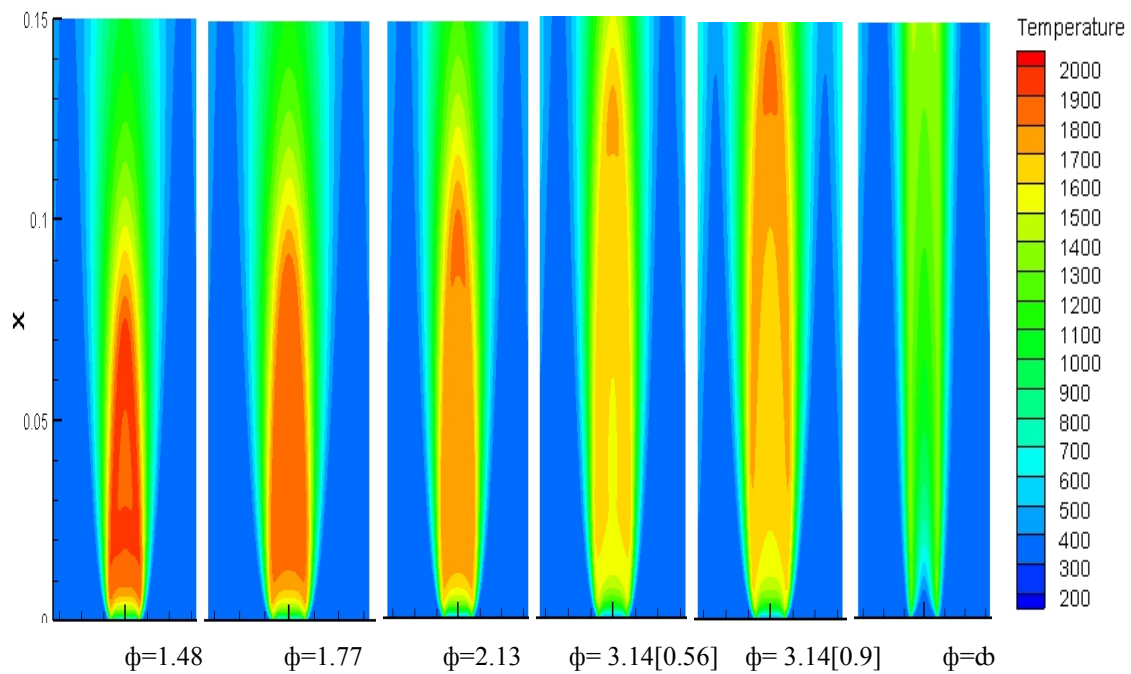


Figure 2. Temperature Contours for Flames for Different Equivalence Ratios

Fig. 2 shows the temperature contours of flames for different equivalence ratios. When the equivalence ratio increases, the flame height is observed to increase. The exact flame height is ascertained from the axial distributions of temperature and different species. The flame height is less for flames having smaller equivalence ratio, because the reaction zone is developed early as more oxygen is available in the mixture. The fuel is consumed within a smaller distance from the burner exit. The premixed flame having least equivalence ratio has reached the maximum temperature.

Two cases (run 4 and 5) having same primary equivalence ratio $\phi=3.14$ with different inlet velocity have been considered to study the effect of velocity on structure of the flames. To keep the equivalence ratio same with different primary jet (air-fuel mixture jet) velocity, the fuel flow rate and the primary air flow rate have been varied. For the flame with the higher primary jet velocity, the flame height and the temperature are more compared to the other flame.

A special case of purely diffusion flame (run 6) has also been taken. The height of this flame is much longer compared to the premixed flames and the tip is not observed within the computational domain. The temperature of this flame is lowest among all the flames.

3.2 Soot Contours

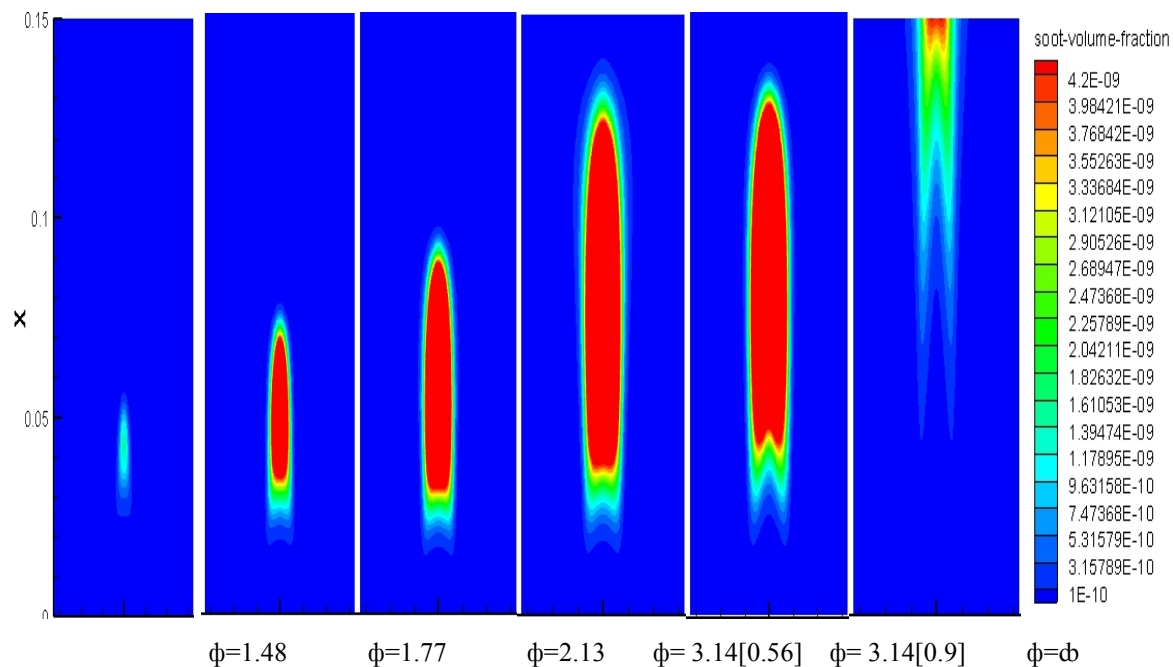


Figure 3. Contours of Soot in the Flames of Different Equivalence Ratios

Contours of soot for different flames are shown in Fig. 3. The soot in the flame of equivalence ratio $\phi=1.48$ is negligibly small and distributed in a very small area along the axis. The soot formation in flames increases with equivalence ratio. Between the two flames having same equivalence ratio, the soot developed in the flame having smaller jet velocity is slightly more. The soot formed in nonpremixed flame is not obtained fully as the entire flame is not within the computational domain considered.

3.3 Temperature Variation Along the Axis

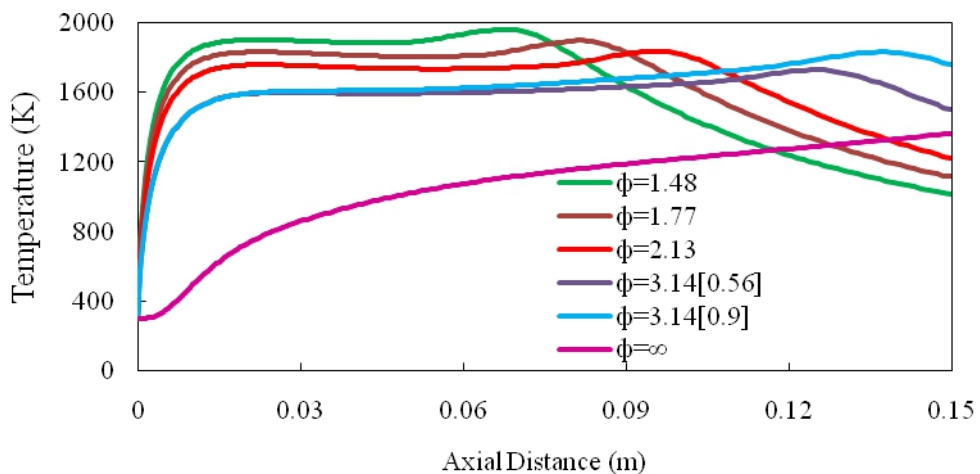


Figure 4. Axial Temperature Distribution for Different Equivalence Ratios

Fig. 4 depicts the temperature variation along the axis of the burner. For all the flames, the temperature at the exit of the burner is same as the atmospheric temperature at which the fuel air mixture enters. Further downstream, the axial temperature increases rapidly from atmospheric temperature as the heat is diffused from

the flame front towards the axis. The temperature increases to the maximum at a certain axial distance where the tip of the flame is located. Further downstream, the temperature decreases because heat is diffused radially outwards. As the equivalence ratio increases, the peak axial temperature is located at a higher distance from the burner exit. This means the flame height is more for higher equivalence ratios. This is also evident from the temperature contours of all the flames (Fig. 2). The overall temperature of the flames is less for lower equivalence ratios. This is because, for flames of lower equivalence ratios, the soot developed in the flames is low (Fig. 3) and less heat is radiated away from the flame. The flame height is smaller for low equivalence ratios and axially stretched more for higher equivalence ratios which is evident from the axial temperature distribution (Fig. 4) as well as from temperature contours (Fig. 2) of different flames. This is because, at lower equivalence ratio, as the stoichiometric condition is reached early after diffusion of oxygen from the secondary stream, the reaction zone is closer to the inlet. For two flames with same equivalence ratio and different velocities, the temperature along the axis is almost same near the burner exit, but at the downstream, the temperature is more for the flame having higher primary jet velocity. This is because of the stretching of the flame height due to higher jet velocity.

For the case of purely diffusion flame, it is observed that for some distance from the burner exit, the temperature does not increase (Fig. 2 and 4) and it gradually increases downstream. At the burner exit, due to absence of air, no combustion can take place. But further downstream, as air is diffused from the secondary stream, the combustion commences and the temperature increases. As only fuel comes through the primary stream, it takes more time to consume the fuel downstream for which the flame is stretched much more beyond the computational domain adopted here. The axial temperature of this flame is the lowest of all as most of the heat is absorbed by the excess fuel.

3.4 Radial temperature distribution at different heights

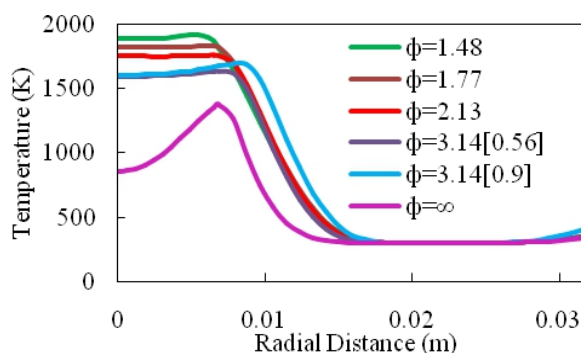


Figure 5. Radial temperature distribution at a flame height of 0.03 m

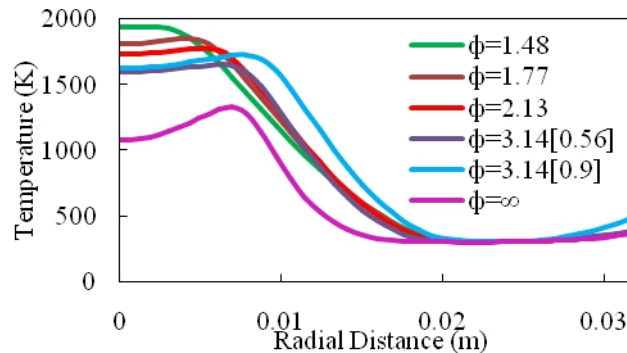


Figure 6. Radial temperature distribution at a flame height of 0.06 m

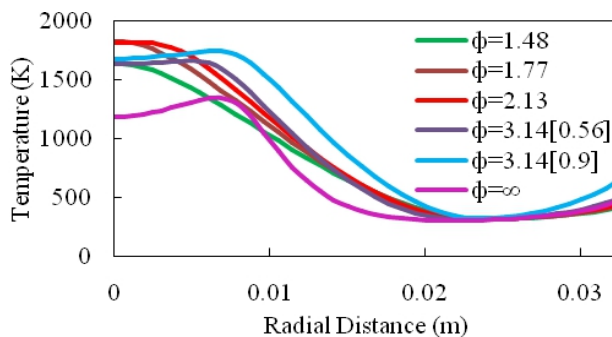


Figure 7. Radial temperature distribution at a flame height of 0.09 m

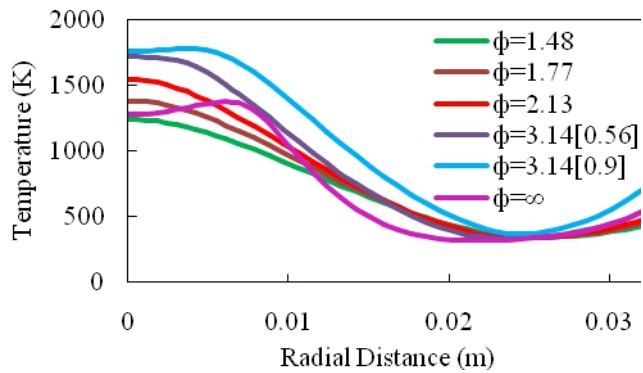


Figure 8. Radial temperature distribution at a flame height of 0.12 m

Fig. 5 shows the radial temperature distribution of flames for different equivalence ratios at a height of 0.03 m from the burner exit. For all flames, as we approach from the outer wall of the burner along radial direction towards the axis, the temperature is constant within the region where secondary air flows at atmospheric temperature. The temperature is somewhat higher near the wall as heat is transferred from the wall to the adjacent layer. As we further approach towards the axis the temperature is gradually increased to a maximum. This is the location where nonpremixed flame is produced. Then the temperature remains almost constant up to the axis of burner. As explained earlier, the flames are stretched more as equivalence ratios is increased. The width of the flame is less for lower equivalence ratios which is also evident from the plot. But the temperature of the flame near the axis is higher for flames of lower equivalence ratios as the stoichiometric condition is reached early. Between the two flames having same equivalence ratios and different primary velocities, the flame having higher primary velocity is stretched more for which the peak temperature is at a higher radial distance compared to the other. For the diffusion flame, the flame is narrow at this height as the flame is extended beyond the computational domain which is explained earlier. This is also observed from the peak temperature of the flame. The temperature is reduced from the peak towards the axis as the heat is absorbed by the fuel flowing in the primary stream. Fig. 6 shows the radial temperature distribution of all flames at a height of 0.06 m from the burner exit. Similar result is also observed here as that obtained at a height of 0.03 m. But the temperature near the wall is increased further since the wall temperature is increased downstream. The width of the flames is observed to be less as flames are closed ones. The difference in temperature of the diffusion flame at the peak and that towards the axis has become less as heat is absorbed by the fuel in the primary stream as it flows downstream. Fig. 7 shows the radial temperature distribution of all flames at a height of 0.09 m from the burner exit. For the flame with lowest equivalence ratio taken in our study, the peak temperature is observed at the axis. So at this height (0.09 m) the tip of the flame is located. Since the stoichiometric condition for other flames is reached after that for the flame of lowest equivalence ratio, the temperature and width of these flames are more. Also as the width of these flames is increased and more heat is transferred from the wall to the secondary air the flat portion of the plot in the secondary air region has become negligible. Fig. 8 shows the radial temperature distribution of all flames at a height of 0.12 m from the burner exit. At this height, the peak temperature of the flame having equivalence ratio 2.13 is observed at the axis. So the tip of this flame is located at this height. So it is obvious that the tip of the flame having equivalence ratio 1.77 is located between 0.09m and 0.12 m. The

temperature of the flames is higher for higher equivalence ratios. Also the temperature of secondary air is increased due to heat received from both sides.

3.5 Axial Distribution of Different Species in a Flame

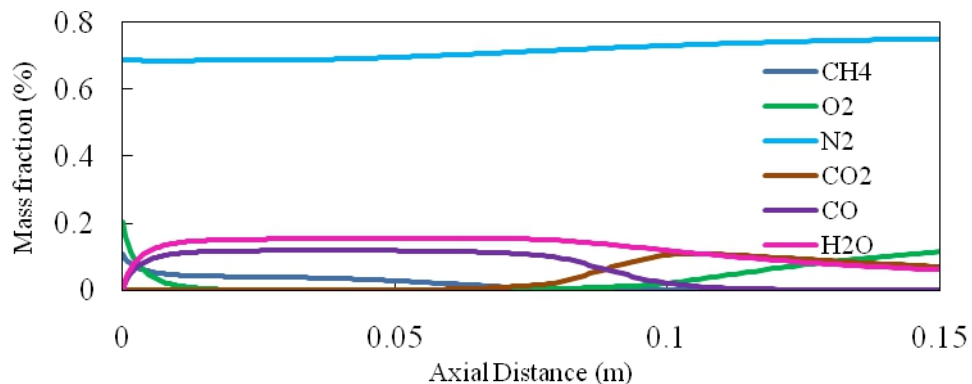


Figure 9. Species Mass Fraction Distribution Along the Axis at $\phi = 2.13$

Fig. 9 shows the axial distribution of mass fraction of all species in the flame at equivalence ratio (ϕ) = 2.13. It is clearly observed that, the mass fraction of methane (CH₄) is the maximum at the exit of the burner and it decreases rapidly within a small distance and then decreases slowly downstream. The flame front is produced at some radial distance from the axis and as fuel is consumed there, the fuel is diffused from the primary stream towards the flame front. The decrease in mass fraction of CH₄ is rather slow afterwards and finally reduces to zero at the tip of the flame. Similarly oxygen is also transported from the primary stream to the flame front and the mass fraction decreases near the inlet towards downstream. However oxygen mass fraction along the axis again increases after reaching to the minimum at the flame tip. It is because beyond the flame tip, oxygen in the secondary air is diffused towards the axis. If we focus on the distribution of CO₂, it is found that, there is no CO₂ mass fraction nearly up to the flame tip. The concentration of CO₂ suddenly increases around the flame tip because of formation of CO₂ at the flame tip. Then mass fraction of CO₂ decreases downstream as it diffuses along radial direction towards the secondary stream. Regarding axial distribution of H₂O and CO concentration, it increases rapidly at the inlet, then remains constant up to the tip of the flame. The H₂O and CO are formed at the flame front and diffused towards the axis. At the inlet concentration of these species is zero for which the diffusion is rapid. After the concentration reaches to a value so that the diffusion of these species is not possible (when equalises with the concentration at the flame front), the concentration along the centreline remains constant up to the flame tip. The concentration of H₂O decreases gradually beyond the flame tip due to radial diffusion whereas the concentration of CO decreases to zero as it is consumed entirely at downstream by reacting with excess air present. N₂ concentration remains same within the flame and gradually increases from the flame tip to the outlet, because the N₂ present in the secondary stream is diffused towards the axis. The axial distribution of all the species for different equivalence ratios are observed to be similar in nature, but the magnitude of concentrations are different which is explained in the following section.

3.6 Axial Distribution of Species in Different Flames

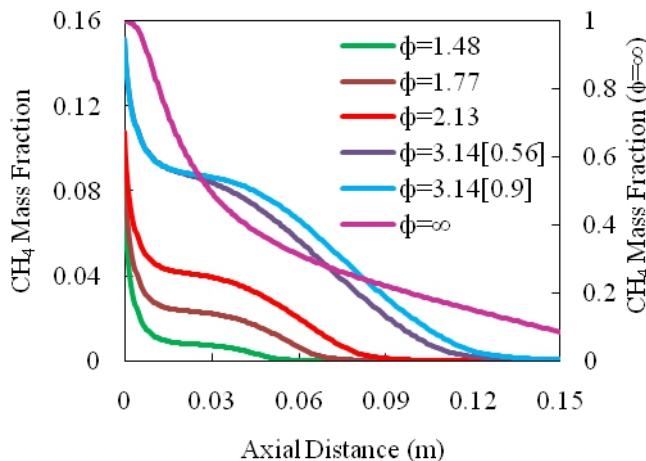


Figure 10. Axial distribution of CH_4 in different flames

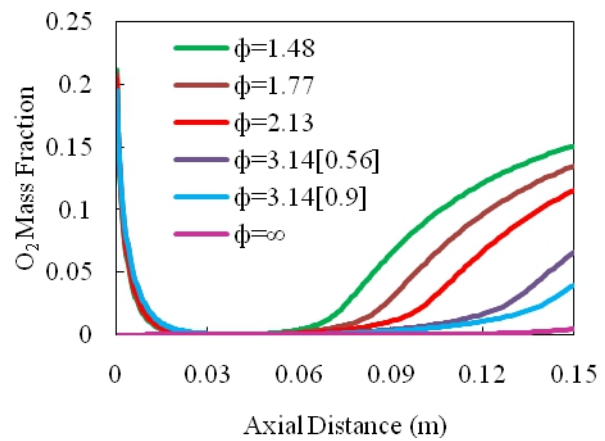


Figure 11. Axial distribution of O_2 in different flames

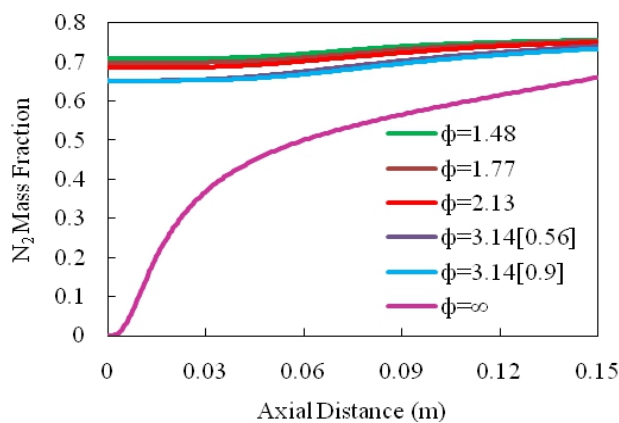


Figure 12. Axial distribution of N_2 in different flames

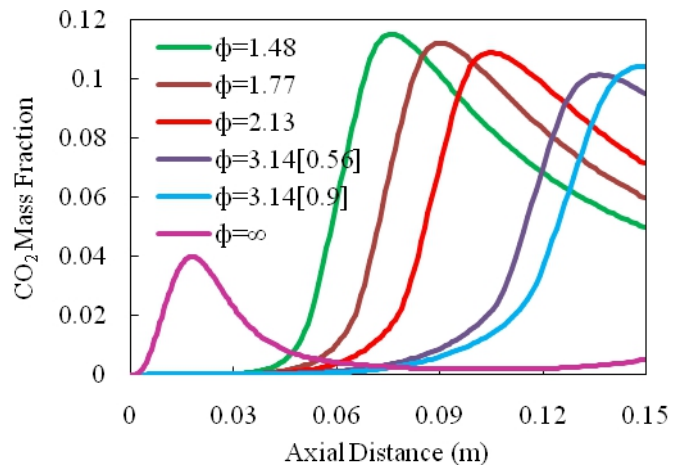


Figure 13. Axial distribution of CO_2 in different flames

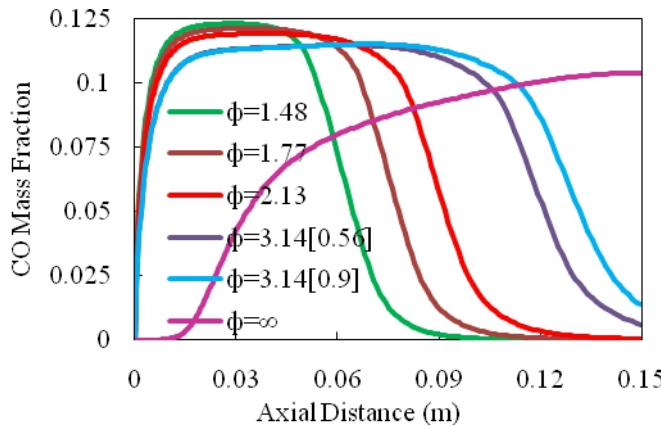


Figure 14. Axial distribution of CO in different flames

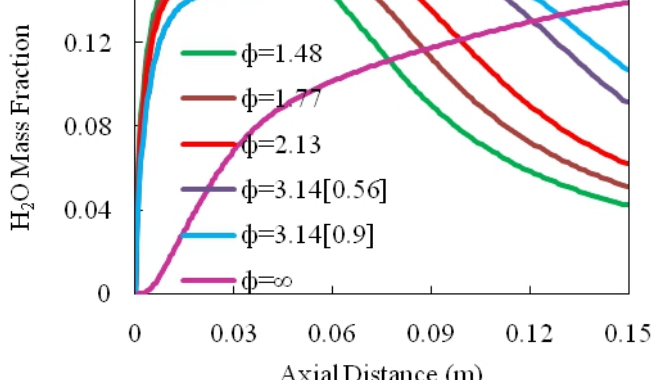


Figure 15. Axial distribution of H_2O in different flames

Axial distribution of methane for different flames is shown in Fig. 10. At the burner exit, the mass fraction of methane is minimum for $\phi = 1.48$ and it is more for other flames as the equivalence ratio is increased. For the nonpremixed flame the mass fraction is maximum (=1) as the primary stream contains only fuel. Along the axial direction the mass fraction decreases to zero at the flame tip as explained earlier. Since the flame height is more



as equivalence ratio increases, the axial location at which mass fraction of the fuel becomes zero is accordingly located. Since the tip of the nonpremixed flame is not located within the computational domain, the mass fraction continuously decreases from the inlet up to the outlet, but has not reached to zero. Fig. 11 shows the axial distribution of oxygen for different flames. At the inlet the mass fraction of oxygen for $\phi = 1.48$ is more and it decreases for flames of higher equivalence ratios. As the difference in mass fraction of oxygen at the inlet is very less, it is not distinguishable from the plot. The concentration of oxygen then decreases to almost zero up to the flame tip and increases thereafter. Since the flame height is different for the flames, the location is observed accordingly. The mass fraction of oxygen along the axis is negligible throughout the computational domain. The axial distribution of nitrogen mass fraction is shown in Fig. 12. For all the premixed flames the mass fraction of N_2 is almost same as there is no consumption of nitrogen at the flame front and there is no diffusion of nitrogen from the axis towards the flame front. The slight increase in N_2 concentration downstream may be attributed to diffusion of N_2 from the secondary stream towards the axis. Though the difference of mass fraction for different flames is very small, the concentration is higher for low equivalence ratio flames throughout the length. Fig. 13 shows axial distribution of CO_2 mass fraction for different flames. For all the premixed flames no CO_2 is observed up to the flame tip and the concentration is suddenly increased at the flame tip and then decreases gradually. As the flame height is different for different flames, the location where concentration of CO_2 increases suddenly is observed accordingly. For the nonpremixed flame, the concentration of CO_2 first increases from the inlet to a peak value and then decreases continuously up to the outlet. Fig. 14 shows the axial distribution of CO for different flames. For different premixed flames the concentration of CO is rapidly increased near the inlet and then remains constant up to the flame tip. Then it decreases to zero beyond the flame tip. As the flame height is different for different flames, the locations of flame tip are observed accordingly. For the diffusion flame, there is no concentration of CO for certain distance near the inlet and the concentration increases gradually up to the outlet. Fig. 15 shows the axial distribution of H_2O of all flames. For all premixed flames, the concentration of H_2O increases rapidly near the inlet and remains constant up to the flame tip and gradually decreases thereafter up to the outlet. For the nonpremixed flame, the concentration of H_2O increases continuously but slowly up to the outlet.

3.7 Radial Distribution of Species and Temperature in the Flame ($\phi = 2.13$)

Fig. 16 shows the radial distribution of different species and temperature at a height of 0.03 m from the burner exit for the flame of equivalence ratio $\phi = 2.13$. The concentration of methane remains constant from the axis to the flame front where the fuel is consumed. So the concentration of fuel deceases gradually to zero which continues outwards as there is no fuel in the secondary stream. The concentration of oxygen in the secondary stream is maximum and same from the outer wall up to the flame front. It is consumed there for which the concentration gradually decreases and the concentration is negligibly small up to the axis.

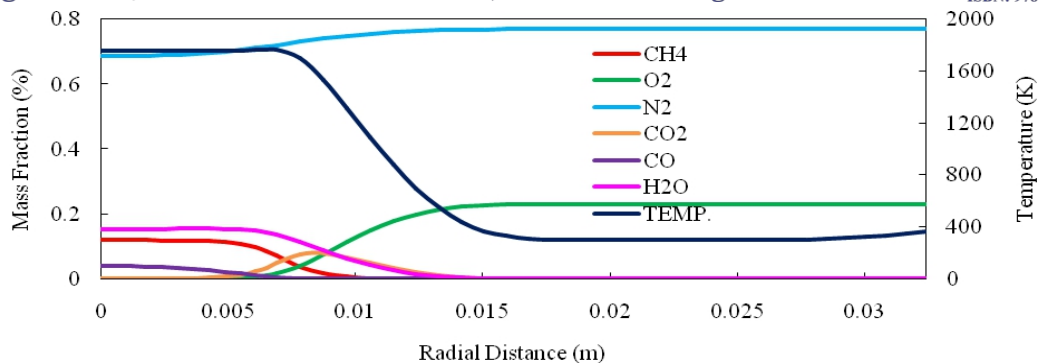


Figure 16. Radial Distribution of Species and Temperature for the Flame ($\phi = 2.13$) at a Height of 0.03 m

The trend of nitrogen concentration is similar to that of oxygen. But the concentration of nitrogen from the flame front up to the axis is slightly less than that in the secondary stream as there is no consumption of nitrogen in the flame front. The concentration of CO_2 peaks at the flame front and decreases on either side because the CO_2 formed at the flame front is diffused to both sides. The CO concentration from the axis to the flame front almost remains same as CO is formed within the flame due to insufficient oxygen there. At the flame front CO is converted to CO_2 as oxygen is diffused from the secondary stream to the flame front. The concentration of H_2O is uniform within the flame as it is produced there. There is no concentration of H_2O in the secondary zone since no oxygen present in the secondary stream. So the concentration of H_2O is decreased gradually at the flame front as we move radially outward. The temperature is maximum within the flame and the magnitude is around 1760K as combustion occurs there. The temperature is gradually decreased to the ambient temperature of 300K in the secondary stream. The temperature is somewhat increased near the wall as some heat is transferred from the wall to the air.

IV. CONCLUSION

- ✓ The flame height increases with increase in equivalence ratio.
- ✓ The formation of soot in the flames is higher with increase in equivalence ratio.
- ✓ The temperature increases to the maximum at a certain axial distance where the tip of the flame is located. Further downstream, the temperature decreases because the heat is diffused radially outward. As the equivalence ratio increases, the peak axial temperature is observed to be at a higher distance from the burner exit.
- ✓ The wall temperature increases with increase in equivalence ratio throughout the length of burner. At lower equivalence ratio the soot formation is less and it increases with increase in equivalence ratio.
- ✓ For all flames, as we approach from the outer wall of the burner along radial direction towards the axis, the temperature is constant within the region where secondary air flows which is at atmospheric temperature. The temperature is somewhat higher near the wall as heat is transferred from the wall to the adjacent layer.
- ✓ For the diffusion flame, the flame is narrow at this height as the flame is extended beyond the computational domain.
- ✓ The mass fraction of methane (CH_4) is the maximum at the inlet of the burner and it decreases rapidly within a small distance and then decreases slowly along the axis downstream.



- ✓ Similarly oxygen (O_2) is also transported from the primary stream to the flame front and the mass fraction decreases at the inlet towards downstream.
- ✓ N_2 concentration remains same within the flame and gradually increases from the flame tip to the exit, because the N_2 present in the secondary stream is diffused towards the axis.
- ✓ We focus on the distribution of CO_2 , it is found that, there is no CO_2 mass fraction nearly up to the flame tip.
- ✓ The H_2O and CO are formed at the flame front and diffused towards the axis. At the inlet concentration of these species is zero for which the diffusion is rapid.
- ✓ At $\phi = 2.13$, The temperature is maximum within the flame and the magnitude is around 1760K as combustion occurs there. The concentration of methane remains constant from the axis to the flame front. The concentration of oxygen in the secondary stream is maximum and same from the outer wall up to the flame front.

REFERENCES

- [1] T. K. Mishra, A. Datta, A. Mukhopadhyaya, "Concentration measurements of selected hydrocarbons in methane/air partially premixed flames using gas chromatography", International Journal of Thermal Sciences vol. 44, pp. 1078-1089, 2005.
- [2] T. K. Mishra, A. Datta, A. Mukhopadhyaya, "Comparison of the structures of methane-air and propane-air partially premixed flames", Fuel, vol. 85, pp. 1254-1264, 2006.
- [3] J. P. Gore and N. J Zhan, "NO emission and major species concentrations in partially premixed laminar methane/air co-flow flames", Combustion Flame, vol. 105, pp. 414-417, 1996.
- [4] Datta, F. Beyrau, T. Seeger, A. Leipertz, "Temperature and concentration measurements in a partially premixed CH₄/air coflowing jet flame using coherent anti-strokes raman scattering", Combustion Science Tech, vol. 176 (11), pp. 1965-1984, 2004.
- [5] V. Mokhov, H. B Levensky, "NO formation in the burnout region of a partially premixed methane/air flame with upstream heat loss", Combustion and Flame, vol. 118, pp. 733-740, 1999.
- [6] A. V. Bennet, C. S. Mcenally, L. D. Pefferle, M. D. Smooke, "Computational and experimental study of axisymmetric coflow partially premixed methane/air flames", Combustion and Flame, vol. 123, pp. 522-546, 2000.
- [7] K. Claramunt, R. Consul, C. D. P. Segarra, A. Oliva, "Multidimensional mathematical modeling and numerical investigation of coflow partially premixed methane/air laminar flames", Combustion and Flame, vol. 137, pp. 444-457, 2004.
- [8] O. Gicquel, P. Miquel, V. Quilichini, M. Hilka, D. Thevenin, N. Darbha, "Numerical and experimental study of NO emission in laminar partially premixed flames", Proceedings of the Combustion Institute, vol. 28, pp. 2419-2425, 2000.
- [9] B. A. V. Bennet, C. S. Mcenally, L. D. Pefferle, M. D. Smooke, "Computational and experimental study of axisymmetric coflow partially premixed ethylene/air flames", Combustion and Flame, vol. 127, pp. 2004-2022, 2001.



IMPACT OF CHEMICALS IN ANTIFOULING PAINTS

ON THE LIFE OF MARINE ORGANISMS

Elias George Kocheemoolayil¹, Mathiazhagan Andy²

¹*Department of Automobile Engineering, SCMS School of Engineering and Technology,*

Vidya Nagar, Palissery, Karukutty, Ernakulam, Kerala, (India)

²*Department of Ship Technology, Cochin University of Science and Technology, Cochin,*

Kerala, (India)

ABSTRACT

The visible appearance of microorganisms such as barnacles, tubeworms, mussels etc on the surface of the marine vessels is only the last stage in the development of biofouling. The development of biofouling is dependent on different factors like the design of the vessel, the coatings applied marine conditions etc. The fouling affects the corrosion resistance. This paper discuss the use of different biofouling agents and its influence on the life of the marine organisms

I. INTRODUCTION

Biofouling accounts for the accumulation of microorganisms, plants, algae, or animals on surface of sea vessels. Antifouling is the ability of specifically designed paints to remove or prevent biofouling on wet surfaces. This kind of fouling can occur on any surface when kept in contact with water. Specifically, the buildup of biofouling on marine vessels develops many problems. It can result in the damage of hull structure. The drag increase can result in decrease speeds by up to 10%, which can require up to 40% increase in fuel consumption. The fuel cost accounts for half of marine transport costs. Antifouling methods are estimated to save the shipping industry around \$60 billion per year. Increased fuel consumption to overcome the drag due to biofouling contributes to adverse environmental effects and is predicted to increase emissions of carbon dioxide and sulfur

dioxide between 38 and 72% by 2020

As the ship travels, marine organisms settle and grow on the bottom and hull of the vessel. These organisms are harmful, because they disturb the anticorrosive paint and thus expose the steel to the sea water. The exposed steel at the bottom starts corroding. So the marine fouling organisms have to be expelled or killed

II. PROTECTION AGAINST BIOFOULING

There are two ways of preventing biofouling one is introducing a smooth surface on which the marine life can not adhere and second is the use of one or more biocides that are released during the life time of the coating which discourage the settlement and growth of marine life. Paints with antifouling agents are used to protect the hulls of the marine vessels, their underwater structures etc. from the fouling caused by marine organisms attached to the surfaces (Debourg et al., 1993). Biofouling can result in roughness of the vessel hulls resulting in increased turbulent flow and drag that reduces the vessel speed per unit of energy consumption (Milne, 1990).



There are both biocide-based and biocide-free antifouling paints .Self polishing technology is another development in this area and it depends on the use of co polymers having self cleaning property .

III. PROBLEMS CAUSED BY THE TOXICITY OF CHEMICALS

Toxic chemicals and heavy metals flow into the ocean from industrial, agricultural, and human wastes runs off or is deliberately discharged into rivers that then empty into the sea. These pollutants cause disease, genetic mutations, birth defects, reproductive difficulties, behavioral changes, and death in many marine organisms. But the severity of the damage varies greatly between species. In many cases, animals near the top of the food chain are most affected because of a process called biomagnification.

Many of the most dangerous toxins settle to the seafloor and it is being consumed by organisms that live or feed on bottom sediments. Because these compounds aren't digested, they accumulate within the animals that ingest them, and become more and more concentrated as they pass along the food chain as animals eat and then are eaten in turn. This is bio magnification, and it means that higher-level predators-fish, birds, and marine mammals-build up greater and more dangerous amounts of toxic materials than animals lower on the food chain. Anti-fouling paints have been relying on toxic chemicals such as tributyltin (TBT), which has been used as in anti-fouling paints on ships,

Tributyltin (TBT) is part of the family of chemicals known as organotins, and has a variety of uses as a pesticide (Sanders, 2008). As the outermost paint layer wears off the ship, new TBT is released in the paint, providing continuous protection from undesirable organisms for up to 4-5 years before it becomes hydrolyzed in seawater (Benson, 1999). TBT is organic nature results in it being rapidly absorbed by organic materials such as bacteria and algae or adsorbed onto suspended particles in water (Benson, 1999). Pesticides such as TBT are toxic to living organisms, farm animals and plants, and humans who are exposed through handling the chemical without adequate protection. It persists in the food chain and bioaccumulates so that any person or animal that eats something contaminated with TBT will be ingesting the toxin. One compound in particular, tributyltinoxide (TBTO), tends to bioaccumulate primarily in the liver and kidneys of organisms, possibly via a protein-binding mechanism.

Lead based and copper based antifouling paints are available and is used but when the concentration exceeds a certain level it also can cause problem for marine organisms . Now research is being concentrated on the use of non toxic coatings form marine applications Impact of these toxic chemicals on the life of marine organism Widespread use of TBT based chemicals in antifouling paints has resulted in elevated ambient concentration of TBT in water adjacent to ship repair facilities .High concentration of TBT in sediments resulted in the damage to cultivated oysters costal dogwhelk , Nucella, and at high concentrations it can lead to suppression of breading activity .In 1980 TBT based antifoulants were banned in European union This ban was closely followed in the United States , Canada and New Zealand . Then In 1990 the Marine Environment Protection Council (MEPC) of the International Maritime Organisation (IMO) called for an international ban of TBT based antifouling agents .



Copper based and lead based antifouling paints Low levels of Copper are a significant threat to salmon and other fish in Puget Sound. Copper interferes with salmon's sense of smell, which reduces their ability to avoid predators, find their way back to their birthplace to spawn, and find mates.

REFERENCES

- [1]. Debourg, C., A. Johnson, C. Lye, L. Tornqvist and C. Unger. 1993. Antifouling products pleasure boats, commercial vessels, nets, fish cages, and other underwater equipment. KEM Report No. 2/93. The Swedish National Chemicals Inspectorate. 58 p.
- [2]. Milne, A., Roughness and drag from the marine paint chemist's viewpoint. Marine Roughness and Drag Workshop Paper 12, London. 1990.
- [3]. Sanders FT. (2008). Reregistration Eligibility Decision for the Tributyltin Compounds:Bis(tributyltin) oxide, Tributyltin benzoate, and Tributyltin maleate (Case 2620). United States Environmental Protection Agency.
- [4]. Benson, Robert. (1999). Tributyltin Oxide. Concise International Chemical Assessment Document 14. World Health Organization; Geneva
- [5]. A Mathiazagan (Ed) 2014 Marine Corrosion and its prevention , Director of public relations and publications , Cochin University of Science and Technology



SUBCONTRACTOR AND VENDOR SELECTION

MODEL USING DATA ENVELOPMENT ANALYSIS

Purnima Bajpai

Research Scholar, Indian Institute of Technology, New Delhi (India)

Assistant Professor, ITM University Gurgaon (India)

ABSTRACT

This paper deals with development of a model for selection of subcontractors and vendors for the construction industry using the data envelopment analysis technique. This paper can also act as an aid to prequalification of vendors and subcontractors and also help in improving the overall efficiency of the subcontractors. The proposed model has also considered an ideal subcontractor or vendor in order to analyze the best possible mechanism that could exist.

Keywords: *Data Envelopment Analysis, Subcontractor, Efficiency, Ideal Vendor*

I. INTRODUCTION

In the Construction Market today the service vendors and the subcontractors have a significant role in execution stage of construction projects. Service vendors & subcontractors help in reducing the direct resource requirement by contractors and also help in providing their specific expertise to the construction projects. In the Indian construction Industry the Contractors heavily rely on the service vendors and subcontractors for execution of the major portion of the works. Hence the occurrence of success or the probability of failure of the projects is subject to their performance.

Therefore the selection of the subcontractors becomes a very crucial element for the decision makers and the management as such decisions need to be taken a number of times during the project life cycle for different services and to ensure that the basic requirements of the project are met.

In this paper the Author has tried to develop a (DEA) Data Envelopment Analysis model in order to help the construction contractors in the process of deciding the appropriate service vendor or subcontractor.

This model would also help in the pre-qualification systems followed by Government Organizations where the qualification in terms of technical, financial capabilities is analysed and used for selection by decision makers.



Table I Literature Review

SR NO	FINDINGS	AUTHORS NAME
1.	Subcontracting of construction work has been a long followed practice in the Indian Construction Industry has and it has been common to sublet almost 80% to % of the construction related works.	(1994) Tracey & Hinze along with Kumaraswamy and Matthews (2000)
2.	Many recent studies have indicated that subletting the construction work has been an important and vital part of the industry and that service vendors and subcontractors continue to play a very important role during the project execution stage of construction projects.	Chotibhongs and Ardit (2005) and Wang and Liu (2005)
3.	The Service vendors and the construction Subcontractors have helped construction contractors to overcome the various problems which relate to the requirement of special skills & expertise, resources and also the shortages of finances	(Elazouni and Metwally, 2000).
4.	Subcontracting and vendor servicing have proven to be much more efficient and economical as compared to projects which have been taken up fully by the contractors without subcontracting.	Arditi and Chotibhongs (2005)
5.	Subcontracting the project works also may help in improving the quality of work produced and also help in reducing the project completion time as well as costs	(Ng et al., 2003).
6.	The subcontractors who are qualified and have the required skill set are able to perform the work in a lesser time and in a more economic manner as compared to general contractors.	(Arditi and Chotibhongs, 2005).
7.	A web based evaluation mechanism for subcontractor was been planned which was coined as WEBSES. WEBSES helps to determine a score for all of the subcontractors under consideration based on a few evaluation criteria roughly around 25 variables were considered that were grouped under 4 heads namely time, cost, quality & safety. All of the 25 variables were assumed to have identical importance.	Arslan et al. (2008)
8.	Data Envelopment analysis is said to be an excellent non-parametric linear programming tool designed specially to appraise the critical efficiency of various Decision Making Units also commonly known as DMUs. These DMUs can either be organization units, businesses, universities, contractors or subcontractors etc.	(Charnes et al., 1978).



The qualitative criterias consist of performance on project's executed in the past with other contractors , the financial capabilities of the subcontractor, timely completion of past projects, HSE records, payment cycle with respect to labor and co supplier etc.

However, none of the existing models give a quantitative combination of the' bid price and the subjective criterias resulting in one all-inclusive subcontractor evaluation model for the construction industry.

II. METHODOLOGY

In general the contractors select the subcontractor based on the lowest bid criteria only that is the ' bid proposal only to make decisions of selection. In order to fill this gap the author of this paper has used the Data Envelopment Analysis (DEA) model to help construction companies in the selection and finalization procedure of subcontractors, keeping in mind the holistic approach.

Table 2 Various Variables Under Consideration for the Data Envelopment Analysis Model for the Vendor/ Subcontractor Selection

VARIABLES UNDER CONSIDERED	MEASUREMENT UNIT OR METHOD OF EVALUATION	INPUTS CONSIDERED	OUTPUTS CONSIDERED
Bid proposed	US Dollar	I	
Performance with respect to past projects	Scale between 1 (lowest) to 10 (highest)		1
Financial capability			2
Timely completion of work in the past			3
Payment to labor within stipulated time			4
Quality of work			5
Workmanship Standard			6
Material Quality			7
Compliance with contractual conditions			8
Compliance with HSE Norms			9
Collaboration with others			10

Table (1) above depicts the various variables that have been considered in the proposed model for selection of subcontractors and the method of measurement.

Keeping in mind the Indian System of subcontracting the Bids are measured and evaluated only in terms of money and the remaining of the variables are measured by interviewing the management and decision makers through a few questions on a selected scale of 1 being the lowest to 10 being the highest.

Keeping in mind the above mentioned selection criteria and methodology and in order to minimize the inputs are minimized and maximize the outputs, the Author has categorized "bid amount proposed" in Table (1) as the

input which needs to be minimized (I) and the remaining of the variables have been considered as outputs (1-10).

The limitation of this method is that its accuracy depends upon the number of decision making units with respect to the number of variables which are being considered as the inputs & outputs respectively.

It is a thumb rule that the bare minimum number of decision making units (DMUs) have to be atleast three times the number of variables under considered .

Fig. 1. Empirical frontier and theoretical frontier.

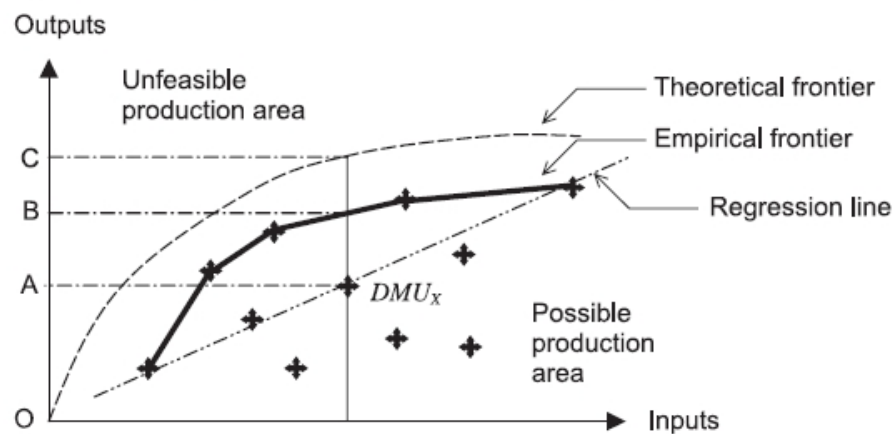
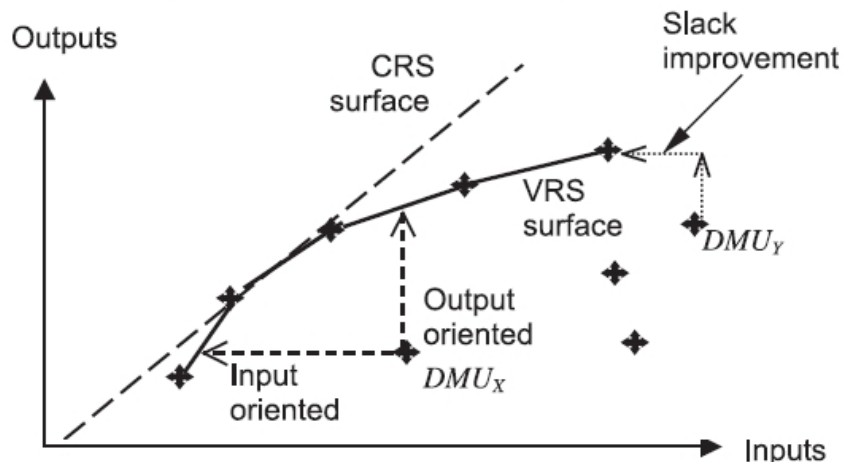


Fig. 2. Envelopment surfaces and orientation.



However based on some of the past studies by Ellis and Wang (2002)(2003) and Cheng. (2007) and other literature has provided a relaxation to this minimum requirement by creating the concept of an ideal decision making unit.

An Ideal decision making unit should have the minimum values of inputs and the corresponding highest values of outputs (2007 Cheng et al.). This same concept has been utilized here in this papers the number of subcontractors or DMU's considered are 10



In this study he Author has considered a total of ten subcontractors for the selection with 1 input (I) and with a total of 10 outputs (measured on a 1-10 scale). These are variables shown in table 1 above. These not only include the bid price proposed but also include various other variables like quality of workmanship, compliance to safety norms, adherence to contractual clauses, financial stability etc in order to give a holistic view to the decision makes and also cover all parameters which are likely to affect the performance of service vendors or subcontractors.

The number of DMUs considered in this study are 10 that are the number of subcontractors and the number of variables under consideration are 11 .Based on the past studies we can say that there are 11 variables, that means that we need a minimum of 33 DMUs in order to keep the inequitable power of DEA intact but since we only have 10 subcontractors, thus the Author has created an Ideal Subcontractor who has the minimum bid price.

After examining the data collected and tabulated in table two (2) we see that the least bid amount proposed has been submitted by Subcontractor no 9 equivalent to \$200,250. Therefore the input value for the considered Ideal Subcontractor should be \$200,250.

Table 3 Data Collected To Conduct Dea

DATA COLECTED											
Subcontractor Number	1	2	3	4	5	6	7	8	9	10	I (\$)
Subcontractor 1	8	6	3	2	4	4	5	9	3	9	2,20,501
Subcontractor 2	4	5	5	8	9	6	5	8	9	8	2,18,622
Subcontractor 3	6	5	8	9	2	9	5	8	3	2	2,26,688
Subcontractor 4	4	6	9	2	1	4	6	7	8	3	2,40,461
Subcontractor 5	1	9	8	6	3	4	6	9	2	1	2,33,589
Subcontractor 6	4	3	4	5	5	7	5	2	1	4	2,14,398
Subcontractor 7	2	3	3	4	3	4	4	1	3	2	213,333
Subcontractor 8	3	5	7	9	2	4	6	7	8	3	241,576
Subcontractor 9	4	6	1	2	3	4	5	4	3	2	\$200,250
Subcontractor 10	5	7	7	8	3	7	5	2	1	4	2,16,815
Ideal Sub	10	10	10	10	10	10	10	10	10	10	\$200,250

**Table 4 Results**

Data Envelopment analysis Results.		
Ranks	Decision Making Units	Efficiency Score Obtained
I	The Ideal Subcontractor	1.00
II	Subcontractor 2	0.86
III	Subcontractor 1	0.85
IV	Subcontractor 3	0.83
V	Subcontractor 5	0.82
VI	Subcontractor 4	0.78
VII	Subcontractor 8	0.77
VIII	Subcontractor 10	0.75
IX	Subcontractor 6	0.69
X	Subcontractor 9	0.55
XI	Subcontractor 7	0.47

Subcontractor1 to Subcontractor 10 have been rated with respect to the Ideal Subcontractor considered by the Author, which has been able to obtain an efficiency score of 1.0. The rest of the Subcontractors have got an efficiency score of less than 1.0.

It is observed that Subcontractor 2 has obtained the highest efficiency score of (0.86) among all of the subcontractors considered.

Thus it is this Subcontractor 2 who shall be selected for the construction work under consideration.

The above data results clearly help to understand that how DEA model can be utilized in order to make the best choice for selecting the best possible vendor or subcontractor out of various potential vendors or subcontractors. As this model not only considers the bid price proposed but also takes into account the various other variables which affect the performance of the vendor or subcontractor and in directly affect the selection criteria as well and are definitely important to ensure proper decision making.

III. CONCLUSIONS

The decision makers in the construction firms depend heavily on the service vendors and subcontractors in order to get the major portion of the construction works executed, hence it is very import for them to get a holistic evaluation method in order to select the best service vendor or subcontractor to get the work done.

For this a bench marking or ranking is essential which has been done through this paper using DEA which combines the important variable of bid price and various other subjective criteria's resulting in a complete evaluation system. Hence this can also act as an important decision making tool. The proposed model through this paper is also very flexible and it can be easily tailored in order to incorporate various other output criteria's depending upon the type of work for which the service vendor or subcontractor has to be selected and also can be altered depending upon the Contractors organizational norms.



- [1]. Charnes A, Cooper W, Rhodes E. Evaluating program and managerial efficiency: an application of data envelopment analysis to program follow through. *ManagSci* 1981;27:668–97.
- [2]. Chiang Y, Cheng E, Tang B. Examining repercussions of consumptions and inputs placed on the construction sector by use of I-O tables and DEA. *Build Environ* 2006;41:1–11.
- [3]. Cooper W, Seiford L, Tone K. Data envelopment analysis: a comprehensive text with models, applications, references and DEAsolver software. Boston/Dordrecht/London: Kluwer Academic Publishers;2000.
- [4]. D. Gerwin and N. J. Barrowman, “An evaluation of research on integrated product development,” *Manag. Sci.*, vol. 48, no. 7, pp. 938–953, Jul. 2002.
- [5]. S. A. Thore and L. Lapao, , S.A. Thore, Ed., “PrioritizingR&D projects in the face of technological and market uncertainty: Combining scenario analysis and DEA,” in *Technology Commercialization: DEA and Related Analytical Methods for Evaluating the Use and Implementation of Technical Innovation*. Boston, MA: Kluwer Academic, 2002,pp. 87–110.
- [6]. R. H. Green, J. R. Doyle, and W. D. Cook, “Preference voting and project ranking using DEA and cross-evaluation,” *Eur. J. Oper. Res.*,vol. 90, no. 3, pp. 461–472, May 1996.
- [7]. A. P. C. Chan and A. P. L. Chan, “Key performance indicators for measuring construction success,” *Benchmarking*, vol. 11, no. 2, pp. 203–221, 2004.
- [8]. T. Cooke-Davies, “The ’real’ success factors on projects,” *Int. J. Project Manag.*, vol. 20, no. 3, pp. 185–190, Apr. 2002.
- [9]. J. P. Lewis, *The Project Manager’s Desk Reference*. New York: Mc- Graw Hill, 2000.
- [10]. A. J. Shenhari, A. Tishler, D. Dvir, S. Lipovetsky, and T. Lechler, “Refining the search for project success factors: A multivariate, typological approach,” *R&D Manag.*, vol. 32, no. 2, pp. 111–126, Mar. 2002.



PROPAGATION OF IONIZING SHOCK WAVE IN A SELF-GRAVITATING NON-IDEAL GAS

B. Nath¹, S. Talukdar²

^{1,2}Assistant Professor, Department of Mathematics, GIMT-Tezpur (India)

ABSTRACT

Propagation of a gas ionizing shock wave in a self-gravitating non-ideal gas in presence of a spatially decreasing azimuthal magnetic field is investigated. The electrical conductivity of the medium ahead of the shock is assumed to be negligible, which becomes infinitely large due to the passage of the shock. The initial density of the gas is assumed to obey a power law. Distribution of the flow variables are obtained in the flow-field behind the shock. Similarity solutions are obtained and effects of variation of the non-idealness parameter, shock Mach number and the variation of initial density exponent are investigated.

Keywords: Magnetogasdynamics, Non-Ideal Gas, Self-Gravitational Effects, Self-Similar Flow, Shock Wave.

I. INTRODUCTION

Shock waves are common in the interstellar medium because of a great variety in supersonic motions and energetic events, such as cloud-cloud collision, bipolar outflow from young protostellar objects, powerful mass losses by massive stars in the late stage of their evolution (stellar winds), super nova explosions, etc. Shock waves are also associated with spiral density waves, radio galaxies and quasars. The explanation and analysis for the internal motion in stars is one of the basic problems in astrophysics. According to observational data, the unsteady motion of a large mass of gas followed by sudden release of energy results in flare-ups in novae and supernovae. A qualitative behavior of the gaseous mass may be discussed with the help of the equations of motion and equilibrium taking gravitational forces into account. Carrus et al.[1] and Sedov [2] have obtained numerical solutions for self-similar adiabatic flows in self gravitating gas, independently. Purohit [3] and Singh and Vishwakarma [4] have discussed homothermal flows behind a spherical shock wave in a self-gravitating gas using similarity method. Shock waves through a variable density medium have been treated by several authors eg. Sakurai [5], Rogers [6], Sedov [2], Rosenau and Frankenthal [7], Nath et. al [8], Vishwakarma and Singh [4] and many others. Their results are more applicable to shocks formed in the deep interior of stars. Recently Nath et. al [10] studied the propagation of magnetogasdynamics shock wave in a self gravitating gas with exponentially varying density. In all of the works mentioned above the medium is taken to be perfect gas.

The assumption that the gas is ideal is no longer valid when the flow takes place at high temperature. The popular alternative to the ideal gas is a simplified van der Waals model. Robert and Wu [11, 12] studied the problem of a spherical implosion by adopting the same van der Waals model. Vishwakarma et. al [13] studied one dimensional unsteady self similar flow behind a strong shock driven out by a cylindrical (or spherical) piston moving in a medium which is assumed to be a non ideal gas obeying simplified van der Waals equation



of state. They have taken the electrical conductivity medium to be infinite. But in many practical cases the medium may be of low conductivity which becomes highly conductive due to the passage of a shock. Such a shock is called a gas-ionizing shock or simply ionizing shock. The propagation of an ionizing shock has been studied by Greenspan [14], Greifinger and Cole [15], Christer [16], Ranga Rao and Ramana [17], Singh [18], Vishwakarma and Singh [19], Singh and Nath [20] in perfect or non-ideal gas.

In the present work we obtain self similar solution for the flow behind a gas ionizing shock wave propagating in a self gravitating non ideal gas in presence of an azimuthal magnetic field. The medium is supposed to have low conductivity which becomes highly conducting due to passage of a strong shock. The initial density of the gas and the initial azimuthal magnetic field are assumed to vary as some power of distance. The total energy of the flow field behind the shock is assumed to be increasing with time due to pressure exerted by a piston or inner expanding surface. The gas ahead of the shock is assumed to be at rest. Effects of variation of shock Mach number, non-idealness parameter and the variation of initial density exponent are investigated.

II. FUNDAMENTAL EQUATIONS AND BOUNDARY CONDITIONS

The fundamental equations governing the unsteady adiabatic spherically symmetric flow of perfectly conducting and self-gravitating gas in which an azimuthal magnetic field is permeated and heat conduction and viscous stress are negligible [10, 21, 22] are:

$$\frac{\partial p}{\partial t} + u \frac{\partial p}{\partial r} + p \frac{\partial u}{\partial r} + \frac{2\rho u}{r} = 0 \quad (1)$$

$$\frac{\partial u}{\partial t} + u \frac{\partial u}{\partial r} + \frac{1}{\rho} \left(\frac{\partial p}{\partial r} + \mu h \frac{\partial h}{\partial r} + \frac{\mu h^2}{r} \right) + \frac{Gm}{r^2} = 0 \quad (2)$$

$$\frac{\partial h}{\partial t} + u \frac{\partial h}{\partial r} + h \frac{\partial u}{\partial r} + \frac{hu}{r} = 0 \quad (3)$$

$$\frac{\partial m}{\partial r} - 4\pi \rho r^2 = 0 \quad (4)$$

$$\frac{\partial e}{\partial t} + u \frac{\partial e}{\partial r} - \frac{p}{\rho^2} \left[\frac{\partial p}{\partial t} + u \frac{\partial p}{\partial r} \right] = 0 \quad (5)$$

where r and t are independent space and time co-ordinates, respectively, u is the fluid velocity, ρ the density, p the pressure, h the azimuthal magnetic field, e the internal energy per unit mass, μ the magnetic permeability, m the mass contained in the sphere of radius r and G is the gravitational constant.

The above system of equations should be supplemented with an equation of state. We assume that the gas obeys a simplified van der Waals equation of state of the form [11, 12, 23, 24]

$$p = \frac{\Gamma \rho T}{1 - b\rho}, \quad e = C_v T = \frac{p(1 - b\rho)}{\rho(\gamma - 1)} \quad (6)$$

where Γ is the gas constant, $C_v T = \frac{\Gamma}{\gamma - 1}$ is the specific heat at constant volume and γ is the ratio of specific heats. The constant b is the van der Waals excluded volume; it places a limit $\rho_{\max} = \frac{1}{b}$, on the density of the gas.



A spherical shock is supposed to be propagating in the undisturbed non-ideal gas with variable density, $\rho = AR^{-\omega}$, $0 \leq \omega < 3$, where A and ω are constants. The azimuthal magnetic field in the undisturbed gas is assumed to vary as $h = BR^{-k}$, $0 < k < 1.5$, where B and k are constants (Rosenau [25]). Also, the gas has negligible electrical conductivity in presence of an azimuthal magnetic field. But due to the passage of the shock, the gas is highly ionized and the electrical conductivity is infinitely large.

The flow variables immediately ahead of the shock front are

$$u_1 = 0, \quad \rho_1 = AR^{-\omega}, \quad h_1 = BR^{-k}$$

$$p_1 = \left[\frac{2\pi GA^2}{(3-\omega)(\omega-1)} + \left(\frac{2-\omega}{\omega-1} \right) \frac{\mu B^2}{2} \right] R^{-2k}, \quad (k = \omega-1) \quad (7)$$

$$m_1 = \frac{4\pi A}{3-\omega} R^{3-\omega}$$

where R is the shock radius and the subscript '1' denotes the conditions immediately ahead of the shock.

The jump conditions at the gas-ionizing shock wave are given by the principles of conservation of mass, momentum, magnetic field and energy [26, 27, 28] are:

$$\left. \begin{aligned} \rho_1 V &= \rho_2 (V - u_2) = m s_1 \\ p_2 - p_1 &= m_s u_2 \\ e_1 + \frac{p_1}{\rho_1} + \frac{1}{2} V^2 &= e_2 + \frac{p_2}{\rho_2} + \frac{1}{2} (V - u_2)^2 \\ h_1 = h_2, \quad m_1 = m_2 \end{aligned} \right\} \quad (8)$$

where subscript '2' denotes the conditions immediately behind the shock front and $V = \frac{dR}{dt}$ denotes the velocity of the shock front.

From equation (8), we get

$$u_2 = (1-\beta)V, \quad \rho_2 = \frac{\rho_1}{\beta}, \quad p_2 = \left[\frac{1}{\gamma M^2} + (1-\beta) \right] \rho_1 V^2, \quad m_2 = \frac{4\pi A}{3-\omega} R^{3-\omega}, \quad h_2 = h_1, \quad (9)$$

where $M = \left(\frac{\rho_1 V^2}{\gamma p_1} \right)^{1/2}$ is the shock Mach number referred to the frozen speed of sound $\left(\frac{\gamma p_1}{\rho_1} \right)^{1/2}$.

The quantity β ($0 < \beta < 1$) is obtained by the relation

$$\beta = \frac{(\gamma-1) + 2\bar{b} + 2M^{-2}}{\gamma+1}. \quad (10)$$

The total energy E of the flow-field behind the shock is not constant, but assumed to be time dependent and varying as [29, 30, 31]

$$E = E_0 t^s, \quad s \geq 0 \quad (11)$$



where E_0 and s are constants. This increase in energy can be achieved by the pressure exerted on the fluid by an expanding surface, which may be, physically, the surface of a stellar corona or condensed explosives or a diaphragm containing a very high-pressure driver gas.

III. SELF-SIMILAR TRANSFORMATIONS

Following the general similarity analysis we define the two characteristic parameters ‘a’ and ‘d’ with independent dimensions as [2]

$$[a] = [A] \quad (12)$$

$$\text{and } [d] = \left[\frac{E_0}{A} \right] \quad (13)$$

The non-dimensional independent variable η in this case will be

$$\eta = \left[\frac{vE_0}{A} \right]^{\frac{1}{(5-\omega)}} rt^{-\delta} \quad (14)$$

$$\text{where } \delta = \frac{2+s}{5-\omega} \quad (15)$$

and v is a constant such that η assume the value ‘1’ at the shock surface. This gives the shock propagation law in the explicit form as:

$$R = \left[\frac{vE_0}{A} \right]^{\frac{1}{(5-\omega)}} t^\delta \quad (16)$$

From this relation, we have

$$\frac{V}{V_0} = \left[\frac{R}{R_0} \right]^{\frac{(\delta-1)}{\delta}} \quad (17)$$

where V_0 and R_0 are the velocity and radius of the shock at the instant of its generation.

We express the fluid variables as

$$u = VU(\eta), \rho = \rho_1 D(\eta), p = V^2 \rho_1 P(\eta), m = \rho_1 R^3 N(\eta), \sqrt{\mu} h_1 = \sqrt{\rho_1} V H(\eta) \quad (18)$$

where U, D, P, N and H are functions of the non-dimensional variable η only.

For the existence of similarity solutions, the shock-Mach number and the Alfvén Mach number should be constants, therefore

$$\delta = \frac{2}{\omega} \text{ and } \omega = \frac{10}{4+s} \quad (19)$$

where $1 < \omega < 2$ ($1 < s < 6$) or $2 < \omega < 2.5$ ($0 < s < 1$).

The equations of motion (1) to (5) can be transformed into a system of ordinary differential equations.

$$(U - \eta) \frac{dD}{d\eta} + D \frac{dU}{d\eta} + \left(\frac{2U}{\eta} - \omega \right) D = 0 \quad (20)$$

$$(U - \eta) \frac{dU}{d\eta} + \left(\frac{\delta-1}{\delta} \right) U + \frac{1}{D} \frac{dP}{d\eta} + \frac{H}{D} \left(\frac{dH}{d\eta} + \frac{H}{\eta} \right) + \frac{G_0 N}{\eta^2} = 0 \quad (21)$$



$$(U - \eta) \frac{dH}{d\eta} + \left(\frac{\delta-1}{\delta} - \frac{\omega}{2} \right) H + H \frac{dU}{d\eta} + \frac{HU}{\eta} = 0 \quad (22)$$

$$\frac{dN}{d\eta} = 4\pi D\eta^2 \quad (23)$$

$$(1 - \bar{b}D)(U - \eta) \frac{dP}{d\eta} - (U - \eta) \frac{\gamma P}{D} \frac{dD}{d\eta} + 2 \left(\frac{\delta-1}{\delta} \right) (1 - \bar{b}D)P + (\gamma - 1 + \bar{b}D)\omega P = 0 \quad (24)$$

where

$$G_0 = \frac{(3-\omega)(\omega-1)}{2\pi} \left[\frac{1}{\gamma M^2} + \frac{\omega-2}{2(\omega-1)} M_A^{-2} \right] \quad (25)$$

and $M_A = \left(\frac{\rho_1 V^2}{\mu h_1^2} \right)^{1/2}$ is the Alfvén Mach number.

From equations (20) to (24), we get

$$\frac{dD}{d\eta} = - \left(\frac{D}{U - \eta} \right) \left[\frac{dU}{d\eta} + \frac{2U}{\eta} - \omega \right] \quad (26)$$

$$\frac{dH}{d\eta} = - \frac{H}{U - \eta} \left[\frac{dU}{d\eta} + \frac{U}{\eta} + \frac{\delta-1}{\delta} - \frac{\omega}{2} \right] \quad (27)$$

$$\frac{dP}{d\eta} = -D \left[\left\{ (U - \eta) - \frac{H^2}{D(U - \eta)} \right\} \frac{dU}{d\eta} + \left(\frac{\delta-1}{\delta} \right) U - \frac{H^2}{D(U - \eta)} \left(\frac{U}{\eta} + \frac{\delta-1}{\delta} - \frac{\omega}{2} \right) + \frac{H^2}{D\eta} + \frac{G_0 N}{\eta^2} \right] \quad (28)$$

$$\frac{dU}{d\eta} = \left[\frac{(1 - \bar{b}D)D(U - \eta)}{H^2(1 - \bar{b}D) + \gamma P - D(1 - \bar{b}D)(U - \eta)^2} \right] \times \left[\begin{aligned} & \left(\frac{\delta-1}{\delta} \right) U - \frac{H^2}{D(U - \eta)} \left(\frac{U}{\eta} + \frac{\delta-1}{\delta} - \frac{\omega}{2} \right) + \frac{H^2}{D\eta} + \frac{G_0 N}{\eta^2} \\ & - \frac{2\gamma P U}{\eta D(1 - \bar{b}D)(U - \eta)} - \left\{ 2 \left(\frac{\delta-1}{\delta} \right) - \omega \right\} \frac{P}{D(U - \eta)} \end{aligned} \right] \quad (29)$$

$$\frac{dN}{d\eta} = 4\pi D\eta^2 \quad (30)$$

Using similarity transformations (18), the shock conditions (9) are transformed into

$$U(I) = (1 - \beta), \quad D(I) = \frac{1}{\beta}, \quad H(I) = M_A^{-1}, \quad P(I) = \left[\frac{1}{\gamma M^2} + (1 - \beta) \right], \quad N(I) = \frac{4\pi}{(3 - \omega)} \quad (31)$$

In addition to the shock conditions (31), the kinematic condition to be satisfied at the inner expanding surface is

given by

$$U(\eta_p) = \eta_p \quad (32)$$

where η_p is the value of η at the inner expanding surface.



IV. RESULTS AND DISCUSSION

The distribution of the flow variables in the flow-field behind the shock front are obtained by numerical integration of the equations (26) to (30) with the boundary conditions (31) by using Runge-Kutta method of fourth order. For the purpose of numerical integration, the values of the constant parameters are taken to be $\gamma = \frac{5}{3}$; $M = 5, 10, 15$; $M_A^{-2} = 0.005, 0.01$; $\bar{b} = 0, 0.05, 0.1$; $\omega = 1.1, 1.2, 1.3$. The value $\bar{b} = 0$ corresponds to the ideal gas case.

The expression for gravitational parameter G_0 is given by equation (25), the exponent in the shock propagation

law δ is given by $\delta = \frac{\omega}{2}$ where ω is the exponent of law of variation of the initial density. Also the exponent in

the law of variation of the total energy behind the shock s is related with ω by $s = \frac{10 - 4\omega}{\omega}$.

Fig 1(a)-1(e) shows the variation of the non-dimensional flow variables U, D, P, H and N with η for different values of \bar{b} and ω and Table 1 shows the density ratio and the position of the inner expanding surface in different cases. Fig 1(a), 1(b), 1(d) shows that the non-dimensional velocity U , density D and mass N increases as we move from the shock front towards the inner expanding surface. Also fig 1(c) shows that the non-dimensional pressure P increases attains a maximum and then decreases rapidly near the inner surface. Fig 1(e) shows that the non-dimensional mass decreases as we proceed towards the inner expanding surface.

Fig 2(a)-2(e) shows the profiles of the non-dimensional flow variables for different values of ω and M^2 and Table 2 shows the variation of the density ratio, the gravitational parameter and the position of the inner expanding surface for different cases.

V. TABLES AND FIGURES

Table 1: Density Ratio β and Position of the Inner Expanding Surface η_p for Different Values

of ω and \bar{b} and $\gamma = \frac{5}{3}$, $M^2 = 5$, $M_A^{-2} = 0.01$.

ω	\bar{b}	β	η_p
1.1	0	0.4000	0.857427
	0.05	0.4375	0.841868
	0.1	0.4750	0.825170
1.2	0	0.4000	0.849694
	0.05	0.4375	0.835003
	0.1	0.4750	0.819260
1.3	0	0.4000	0.841013
	0.05	0.4375	0.827580
	0.1	0.4750	0.813081

Table 2: Density Ratio β , Position of the Inner Expanding Surface η_p and Gravitational Parameter

G₀ for Different Values of ω and M² and $\gamma = \frac{5}{3}$, $\bar{b} = 0.1$, M_A⁻² = 0.005

ω	M ²	β	G ₀	η_p
1.1	5	0.475	0.00294835	0.825261
	10	0.400	0.00113398	0.855662
	15	0.375	0.00052919	0.865493
1.2	5	0.475	0.00630254	0.819299
	10	0.400	0.00286497	0.851303
	15	0.375	0.00171887	0.861644
1.3	5	0.475	0.00926680	0.813063
	10	0.400	0.00439666	0.846797
	15	0.375	0.00277327	0.857691

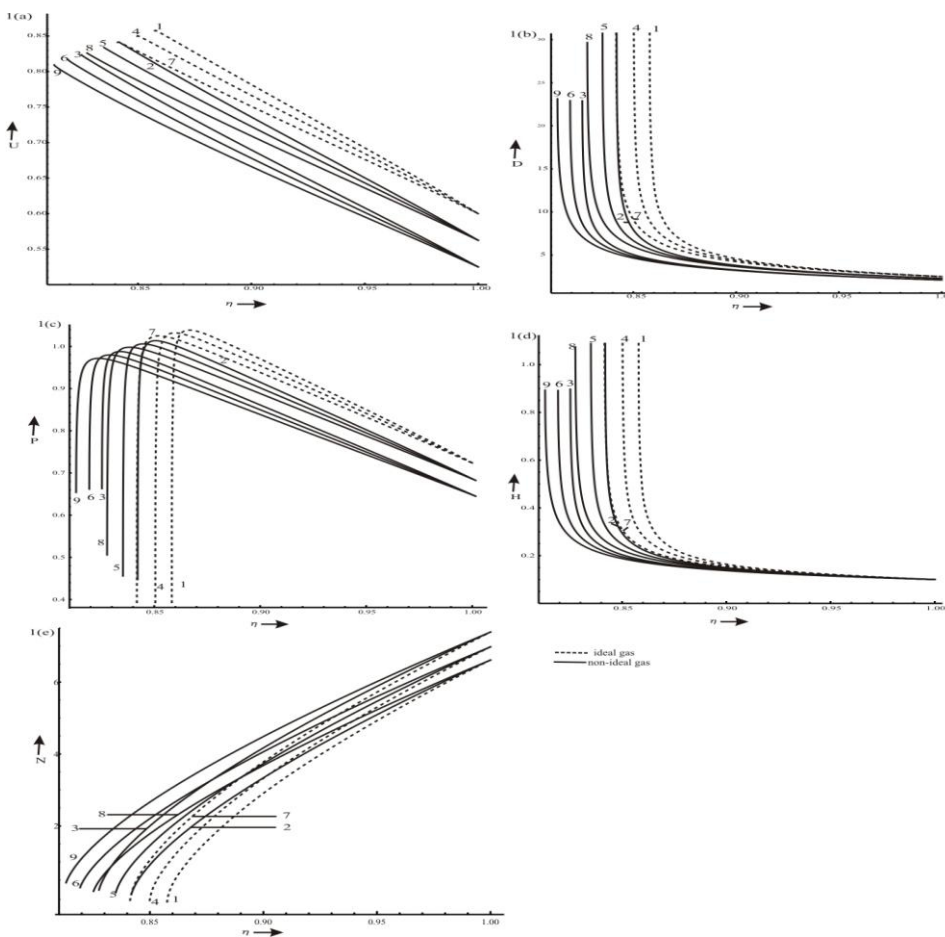


Fig 1: Variation of non dimensional flow variables for different values of (a) velocity, (b) density, (c) pressure, (d) magnetic field and (e) mass

1. $\omega = 1.1, \bar{b} = 0$; 2. $\omega = 1.1, \bar{b} = 0.05$; 3. $\omega = 1.1, \bar{b} = 0.1$; 4. $\omega = 1.2, \bar{b} = 0$; 5. $\omega = 1.2, \bar{b} = 0.05$; 6. $\omega = 1.2, \bar{b} = 0.1$;

7. $\omega = 1.3, \bar{b} = 0$; 8. $\omega = 1.3, \bar{b} = 0.05$; 9. $\omega = 1.3, \bar{b} = 0.1$;

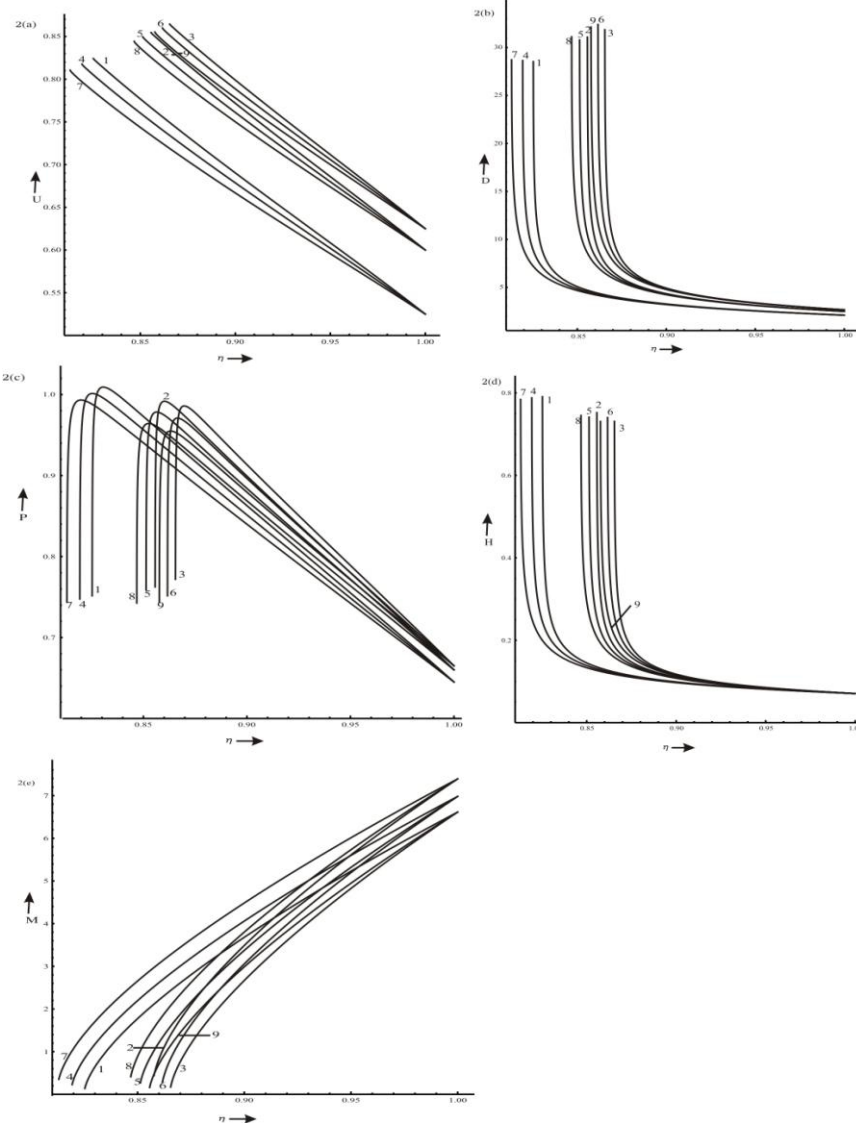


Fig 2: Variation of non dimensional flow variables for different values of (a) velocity, (b) density, (c) pressure, (d) magnetic field and (e) mass

1. $\omega = 1.1, M^2 = 5$; 2. $\omega = 1.1, M^2 = 10$; 3. $\omega = 1.1, M^2 = 15$; 4. $\omega = 1.2, M^2 = 5$; 5. $\omega = 1.2, M^2 = 10$;

6. $\omega = 1.2, M^2 = 15$; 7. $\omega = 1.3, M^2 = 5$; 8. $\omega = 1.3, M^2 = 10$; 9. $\omega = 1.3, M^2 = 15$;

It is found that:

The effects of an increase in the value of the non-idealness parameter \bar{b} are:

1. To increase the value of β ; to decrease the shock strength (see Table 1)
2. To increase the distance of the inner expanding surface from the shock front. Physically it means that the gas behind the shock is less compressed. (see Table 1)
3. To decrease the non-dimensional velocity U , density D , magnetic field H and pressure P . (Fig 1(a)—1(d))
4. To increase the non-dimensional mass N . (Fig 1(e))

The effects of an increase in the exponent of the density variation ω are:



1. To increase the distance of the inner expanding surface from the shock front (see table 1 and 2).
2. To decrease the velocity U, density D, magnetic field H, pressure P and to increase the mass N at any point in the flow-field behind the shock. (see Fig 1(a)-(e), 2(a)-(e))
3. To increase the value of the parameter of gravitation G_0 (see Table 2).

The effects of an increase in the value of the shock Mach number M, are:

1. To decrease the value of β (see Table 2).
2. To decrease the distance of the inner expanding surface from the shock front (see Table 2).
3. To increase the non-dimensional velocity U, density D, pressure P, magnetic field and to increase the non-dimensional mass N. (see Fig 2(a)—2(e))
4. To decrease the value of the parameter of gravitation G_0 (see Table 2)

REFERENCE

- [1]. P. A. Carrus. , P. A. Fox., F. Hass and Z. Kopal, The propagation of shock waves in a stellar model with continuous density distribution. *Astrophys. J.*, 113, 1951, 496-518.
- [2]. L. I. Sedov, *Similarity and dimensional methods in mechanics*, (Academic Press, New York. Chapter IV, 1959).
- [3]. S. C. Purohit, Self-similar homothermal flow of self-gravitating gas behind shock wave. *J. Phys. Society (Japan)*, 36, 1974, 288-292.
- [4]. J. B. Singh, Self-similar ionizing shock waves with radiation heat flux, *Indian Journal of Technology*, 21, 1983, 315-318.
- [5]. A. Sakurai Propagation of spherical waves in stars. *J. Fluid Mech.*, 14, 1956, 436-453.
- [6]. M. H. Rogers, Analytic solutions for the blast-waves problem with an atmosphere of varying density, *Astrophys. J.*, 125, 1957, 478-493
- [7]. P. Rosenau and S. Frankenthal, Equatorial propagation of axisymmetric magnetohydrodynamic shocks, *Phys. Fluids*, 19, 1976a, 1889-1899.
- [8]. O. Nath, S. N. Ojha and H. S. Takhar, A study of stellar point explosion in a self-gravitating radiative magneto-hydrodynamic medium, *Astrophys. Space Sci.*, 183, 1991, 135-145,
- [9]. J. P. Vishwakarma and A. K. Singh, A self-similar flow behind a shock wave in a gravitating or non-gravitating gas with heat conduction and radiation heat flux, *J. Astrophys. Astron.*, 30, 2009, 53-69
- [10]. G. Nath, J. P. Vishwakarma, V. K. Srivastava and A. K. Sinha, Propagation of a magnetogasdynamics shock waves in a self-gravitating gas with exponentially varying density, *J. Theo. Appl. Phys.*, 7, 2013, 15.
- [11]. P. H. Roberts and C. C. Wu, Structure and stability of a spherical implosion, *Phys. Lett. A*, 213, 1996, 50-64



- [12]. P. H. Roberts and C. C. Wu, The shock wave theory of sonoluminescence. In Shock socussing effects in medical science and sonoluminescence, Edited by R.C. Srivastava, D. Leutloff, K. Takayama and H. Groning, (Springer-Verlag, Heidelberg, 2003).
- [13]. J. P. Vishwakarma, A. K. Maurya and K. K. Singh, Self-similar adiabatic flow headed by a magnetogasdynamics cylindrical shock wave in a rotating non-ideal gas, *Geo. Astro. Fluid Dyn.*, 101(2), 2007, 155-168.
- [14]. H. P. Greenspan, Similarity solution for a cylindrical shock magnetic field interaction, *Phys. Fluids*, 5, 1962, 255-259
- [15]. C. Greinfinger and J. D. Cole, Similarity solution for cylindrical magnetohydrodynamic blast waves, *Phys. Fluids* 5, 1962, 1597-1607
- [16]. A. H. Christer, Self-similar cylindrical ionizing shock and detonation waves, *Z Angew Math. Mech.* 52, 1972, 11-22.
- [17]. M. P. Rangarao and B. V. Ramana, Self-similar cylindrical magnetogasdynamics and ionizing shock waves. *Indian Int. J Engng. Sci.*, 11, 1973, 337-351.
- [18]. J. B. Singh and P. R. Vishwakarma, Self-similar solutions in the theory of flare-ups in novae I, *Astrophys. Space Sci.*, 95, 1983, 94-104.
- [19]. J. P. Vishwakarma and M. Singh, Ionizing cylindrical shock waves in a rotating homogeneous non-ideal gas. *Int. J. Mech. Appl.* 2(2), 2012, 14-23.
- [20]. K. K. Singh and B. Nath, Self-similar cylindrical ionizing shock wave in a rotating axisymmetric gas flow. *Indian J. Sci. Tech.*, 2013.
- [21]. G. B. Whitham, On the propagation of shock wave through regions of non-uniform area or flow. *J. Fluid Mech.*, 4, 1958, 337-360.
- [22]. J. P. Vishwakarma and G. Nath, Cylindrical shock wave generated by a piston moving in a non-uniform self-gravitating rotational axisymmetric gas in the presence of conduction and radiation heat flux, In Petrova VM (ed) *Advances in Engineering Research*, Nova, Hauppauge, 2011, 537-576.
- [23]. K. K. Singh and B. Nath, Self-similar flow of a non-ideal gas with increasing energy behind a magnetogasdynamics shock wave under a gravitational field, *J Theo. Appl. Mech.*, 49(2), 2011, 501-513
- [24]. G. Nath, Shock wave generated by a piston moving in a non-ideal gas in the presence of a magnetic field: Isothermal flow, *South East Asian J. Math Math. Sci.*, 5, 2007, 69-83.
- [25]. P. Rosenau, Equatorial propagation of axisymmetric magnetohydrodynamic shocks II. *Physics of Fluids*, 20, 1977, 1097-1103.
- [26]. J. B. Singh and S. K. Srivastava, Cylindrical ionizing shock waves in a non-ideal gas, *J. Purv. Acad. Sci., Jaunpur* 2, 1991, 39-46.



- [27]. J. P. Vishwakarma and S. N. Pandey, Converging cylindrical shock waves in a non-ideal gas with an axial magnetic field, Def. Sci. J., 56, 2006, 721-731.
- [28]. J. P. Vishwakarma and M. Singh, Self-similar cylindrical ionizing shock waves in a non-ideal gas with radiation heat-flux, Appl. Math. 2, 2012, 1-7.
- [29]. M. H. Rogers, Similarity flows behind strong shock waves, Quart. J. Mech. Appl. Math XI(11), 1958, 411-422.
- [30]. R. A. Freeman, Variable energy blast waves, J. Phys. D., 1, 1968, 1697-1710.
- [31]. M. N. Director and E. K. Dabora, An experimental investigation of variable energy blast waves, Acta Astronaut, 4, 1977, 391-407.